1

SAINT PETERSBURG STATE UNIVERSITY STUDIES IN PHYSICS

Vladimir A. Chirkov

Influence of Charge Formation Mechanism on the Structure of Electrohydrodynamic Flow in Highly Non-Uniform Electric Field

Saint Petersburg | 2013

The series *Saint Petersburg State University Studies in Physics* presents final results of research carried out in postgraduate biological programs at St. Petersburg State University. Most of this research is here presented after publication in leading scientific journals.

The supervisors of these works are well-known scholars of St. Petersburg State University and invited foreign researchers. The material of each book has been considered by a permanent editorial board as well as a special international commission comprised of well-known Russian and international experts in their respective fields of study.

Printed in Russia by St. Petersburg University Press
11/21 6th Line, St. Petersburg, 199004

ISSN 2308-6599
ISBN 978-5-288-05452-5

ABSTRACT

Chirkov, Vladimir A.
Influence of Charge Formation Mechanism on the Structure of Electrohydrodynamic Flow in Highly Non-Uniform Electric Field
Saint Petersburg: Saint Petersburg State University, 2013, 51 p. (+included articles)
Saint Petersburg State University Studies in Physics, Vol. 1

This work presents the original results of investigations of electrohydrodynamic (EHD) flows and current passage processes in low-conducting liquids. The corresponding phenomena are very complicated and, so, to gain more insight into EHD flow behavior, the research was conducted on the base of both computer simulation and experimental study. The major part of the investigation was made for the needle–plane electrode system where the electric field distribution is highly non-uniform, which considerably enhances the near-electrode processes of charge formation even at relatively low voltage across the interelectrode gap.

A new method for computer simulation of EHD flows on the basis of the complete set of electrohydrodynamic equations was developed. Among other things, it allows calculating electroconvection processes in the case of charge injection into liquid with non-zero conductivity and computing the integral current characteristics. In turn, it lets one investigate features of EHD flow without disregarding the dissociation and recombination processes in the bulk, as well as make a comparison of the calculated current with the experimental one.

The proposed simulation technique provided a framework for comprehensive and systematical research into high-voltage processes of the current passage through dielectric liquids in a wide voltage range (up to the breakdown). EHD flow behavior was studied in different cases of charge formation: injection into non-conducting liquid, dissociation without injection, injection into low-conducting liquid and field-enhanced dissociation. Performed numerical calculations allowed us to describe kinematic, force and electric current structures of EHD flows and investigate the influence of charge formation mechanisms on them. It was shown that both injection and dissociation mechanisms of charge formation can lead to emergence of EHD flows with the same direction, similar structure and intensity. A part of obtained results was compared with the original experimental data and a satisfactory qualitative and quantitative agreement was observed.

The transient regime of EHD flow formation was considered and corresponding unsteady integral current characteristics were calculated. The computer simulation made it possible to explain the features of current–time characteristics and to show that their shape is dependent on mechanisms of charge formation, the ratio of the initial and steady-state ion concentrations, and the mechanisms of charge transport. The relation between stages of EHD flow formation and sections of unsteady integral current characteristics was revealed. Calculated current–time characteristics were shown to be in agreement with the aggregate of various experimental data presented in the literature.

Keywords: computer simulation; low-conducting liquid; injection; conduction; field-enhanced dissociation; current characteristics; high-voltage processes

Supervisor Professor Yury K. Stishkov
Department of Radiophysics
Faculty of Physics
St. Petersburg State University, Russia

Opponents

Professor Nikolai V. Egorov (Chairman)
Head of Department of Modelling of Electromechanical and Computer Systems
Faculty of Applied Mathematics and Control Processes
St. Petersburg State University, Russia

Professor Andrey N. Klyucharev
Department of Optics
Faculty of Physics
St. Petersburg State University, Russia

Professor Valeriy A. Pavlov
Department of Radiophysics
Faculty of Physics
St. Petersburg State University, Russia

Professor Vitaly A. Polyansky
Laboratory of Physical Chemical Hydrodynamics
Institute of Mechanics
M.V. Lomonosov Moscow State University, Russia

Professor Anatoly I. Zhakin
Department of General and Applied Physics
Faculty of Innovation and Management
Southwest State University, Russia

Professor Jerzy Mizeraczyk
Head of Centre For Plasma And Laser Engineering
Institute of Fluid-Flow Machinery
Polish Academy of Sciences, Poland

Dr. Dantchi Koulova
Department of Fluid Mechanics
Institute of Mechanics
Bulgarian Academy of Sciences, Bulgaria

ACKNOWLEDGEMENTS

First of all, I would like to express my sincere gratitude to my supervisor Prof. Yury K. Stishkov, who has guided and taught me during the last ten years, for his support and invaluable assistance. I am grateful to the team of *Electrophysics* research and education center for their collaboration and fruitful discussions of the results. Special thanks to my elder colleagues Vyacheslav Dernovsky, Ilya Elagin, and Aleksander Buyanov for their assistance and to Sergei B. Afanasyev for his help in making my first experimental set-up. I am grateful to Tavrida Electric for its collaboration with my department and providing us with up-to-date equipment. The participation in conferences abroad would be impossible without great assistance of my English teacher Valery A. Koptyaev.

I would like to express my gratitude to Prof. Huber Romat who was the Chairman of 16th International Conference on Dielectric Liquids that was my first conference abroad and where I got the award for the best student presentation. It was the key point in my career and powerful incentive to continue research.

I would like to extend my thanks to my parents Irina and Mikhail Gaponyuk and my bride Anna Pronevich for their real support and patience.

Research was carried out using computer resources provided by Resource Center "Computer Center of SPbU".

Financial support was provided by Saint Petersburg State University (Russia) and Russian Foundation for Basic Research.

LIST OF FIGURES

FIGURE 13 (a) The current–voltage characteristics and (b) the velocity distributions along the cross-section through the middle of the interelectrode gap obtained in the experiment and in the simulation at the voltage of 15 kV.

FIGURE 14 The contour plot of velocity obtained in the experiment (on the left-hand side) and in the simulation (on the right-hand side) at the voltage of 12 kV.

NOMENCLATURE

Symbol	Description	Units
A	the first injection coefficient	[1/m^2]
A_{Coul}	density of the work of the viscous force leading to dissipation	[N/m^2]
A_{frict}	density of work of the Coulomb force	[N/m^2]
B	the second injection coefficient	[V/m]
b	ion mobility	[m^2/V s]
D	diffusion coefficient	[m^2/s]
d	function of charge loss	[1/m^2]
$\vec{E}$	electric field	[V/m]
e	elementary electric charge	[C]
F	relative enhancement of the dissociation intensity	
$\vec{\mathcal{F}}_{\mathrm{Coul}}$	density of the Coulomb force	[N/m^3]
$\vec{\mathcal{F}}_{\mathrm{frict}}$	density of the friction force	[N/m^3]
f	injection function	[1/m^2]
f_{E}	weighting electric field	[1/m]
g	source function	[1/m^3 s]
h	cell height	[m]
I	total current	[A]
I_1	modified Bessel function of the first kind	
i	subscript indicating ion species	
$\vec{J}$	density of ion flux	[1/m^2 s]
$\overrightarrow{J_{\mathrm{el}}}$	electric current density	[A/m^2]
k_{B}	Boltzmann constant	[J/K]
L	length of the interelectrode gap	[m]
N	outward normal	
n	ion concentration	[1/m^3]
P	hydrodynamic pressure	[Pa]
R	cell radius	[m]
r	*r*-coordinate	[m]
r_1	needle tip radius	[m]
r_2	needle base radius	[m]
T	temperature	[K]
t	time	[s]
$\vec{u}$	fluid velocity	[m/s]
V	cell volume	[m^3]
W	Energy density	[J/m^3]
Z	ion valence	
z	*z*-coordinate	[m]
γ	mass density	[kg/m^3]
ε	relative electric permittivity	
ε_0	electric constant	[F/m]
η	dynamic viscosity of fluid	[Pa s]

ρ	space charge density	[C/m^3]
σ_0	low-voltage conductivity	[S/m]
σ'	momentum flux	[J/m^3]
σ'_{ik}	viscous stress tensor	[J/m^3]
φ	electric potential	[V]

CONTENTS

LIST OF INCLUDED ARTICLES

PI Stishkov, Yu. K. and Chirkov, V. A. 2008. Computer simulation of EHD flows in a needle-plane electrode system. *Tech. Phys.*, 53(11), 1407–1413.

PII Stishkov, Yu. K. and Chirkov, V. A. 2012. Formation of electrohydrodynamic flows in strongly nonuniform electric fields for two charge-formation modes. *Tech. Phys.*, 57(1), 1–11.

PIII Stishkov, Yu. K., Krasil'nikov, S. Yu., and Chirkov, V. A. 2012. Investigation of electrohydrodynamic flows in superstrong electric fields. *Surf. Eng. and Appl. Electrochemistry*, 48(4), 312–317.

PIV Chirkov, V. A. and Stishkov, Yu. K. 2013. Current-time characteristic of the transient regime of electrohydrodynamic flow formation. *J. Electrostatics*, 71(3), 484–488.

OTHER PUBLICATIONS

AI Stishkov, Yu. K. and Chirkov, V. A. 2013. Peculiarities of the structure of near-electrode dissociation-recombination layers at different levels of low-voltage conductivity of weakly conducting liquid. *Technical Physics*, 58(12), *In press*.

AII Stishkov, Yu. K., Chirkov, V. A., and Sitnikov, A. A. 2013. Dynamic current-voltage characteristics of weakly conducting liquids in highly non-uniform electric field. *Surf. Eng. and Appl. Electrochemistry*, 49(6), *In press*.

AIII Stishkov, Y. and Chirkov, V. 2011. Dependence of the electrohydrodynamic flows structure in very non-uniform electric field on the charge formation mechanism. In *Proc. of the 17th International Conference on Dielectric Liquids, Trondheim, Norway*.

AIV Stishkov, Yu. K. and Chirkov, V. A. 2008. Features of electrohydrodynamic flows in needle–plane electrode system. In *Proc. of the 16th International Conference on Dielectric Liquids, Poitiers, France*, 33–35.

AV Chirkov, V. A. and Stishkov, Yu. K. 2012. Electrohydrodynamic mechanism of the electric conduction. In *Proc. of the International Symposium on Electrohydrodynamics, Gdansk, Poland*, 56–61.

AVI Stishkov, Yu. K., Zuev, D., Vinaykin, M., and Chirkov, V. 2009. Comparison of EHD-flows in point-point and point-plane electrode systems. In *Proc. of the International Symposium on Electrohydrodynamics, Sarawak, Malaysia*.

AVII Stishkov, Yu. K. and Chirkov, V. A. 2010. Structural features of EHD flows in asymmetric electrode systems. *Vestnik Sankt-Peterburgskogo Universiteta Ser. 4 (Physics and Chemistry)*, 1, 36–50. [in Russian with English summary]

AVIII Afanasyev, S. B., Lavrenyuk, D. S., Nikolaev, P. O., Pavleino, M. A., Stishkov, Yu. K., and Chirkov, V. A. 2009. A semiautomatic method for computer processing of group motion characteristics of objects and different nature flows. *Vestnik Sankt-Peterburgskogo Universiteta Ser. 10 (Applied Mathematics, Informatics, Control Processes)*, 1, 3–13. [in Russian with English summary]

AIX Stishkov, Yu. K. and Chirkov, V. A. 2012. Current–time characteristics of the transient regime of electrohydrodynamic flow formation for different models of charge formation. In *Proc. of 10th Intern. Conf. on Modern Problems of Electrophysics and Electrohydrodynamics of Liquids*, *MPEEL´12*, St. Petersburg, Russia, 82–85. [in Russian with English summary]

AX Stishkov, Yu. K., Chirkov, V. A., and Sitnikov A. A. 2012. Dynamic current-voltage characteristics of weakly conducting liquids in highly non-uniform electric field. In *Proc. of 10th Intern. Conf. on Modern Problems of Electrophysics and Electrohydrodynamics of Liquids*, *MPEEL´12*, St. Petersburg, Russia, 164–167. [in Russian with English summary]

AXI Stishkov, Yu. K. and Chirkov, V. A. 2009. Features of convective mechanism of high-voltage conductivity in needle–plane system. In *Proc. of 9th Intern. Conf. on Modern Problems of Electrophysics and Electrohydrodynamics of Liquids*, *MPEEL´09*, St. Petersburg, Russia, 71–76. [in Russian]

AXII Stishkov, Yu. K., Chirkov, V. A., and Ageev, A. V. 2012. Features of dissociation EHD-pump operation in highly non-uniform electric field. In *Proc. of 13th Intern. Scien.-Pract. Conf. "Basic and Applied Researches, Development and Application of High Technologies in Industry and Economy"*, St. Petersburg, Russia, 2/1, 187–189. [in Russian]

AXIII Stishkov, Yu. K., Kozub., V. A., and Chirkov, V. A. 2010. Computer simulation and optimization of electrohydrodynamic pump. In *Proc. of 9th Intern. Scien.-Pract. Conf. "Basic and Applied Researches, Development and Application of High Technologies in Industry and Economy"*, St. Petersburg, Russia, 4, 326–330. [in Russian]

AXIV Elagin, I. A., Stishkov, Yu. K., Chirkov, V. A., and Glushchenko, P. V. 2008. Computer simulation of processes of natural convection and EHD flows in symmetrical systems of heaters-electrodes. In *Proc. of 13th Plyos Intern. Conf. on Nanodispersed Magnetic Fluids*, Plyos, Russia, 227–235. [in Russian]

AXV Stishkov, Yu. K. and Chirkov, V. A. 2006. Features of zone structure of EHD flows in needle over plane system. In *Proc. of 8th Intern. Conf. on Modern Problems of Electrophysics and Electrohydrodynamics of Liquids*, *MPEEL´06*, St. Petersburg, Russia, 175–179. [in Russian]

AXVI Stishkov, Yu. K. and Chirkov, V. A. 2011. Simulation of current–voltage characteristics below and above the threshold of EHD flow onset. In *Proc. of 3th All-Russian. Conf. "Physicochemical and applied problems of magnetic dispersed nanosystems"*, Stavropol, Russia, 233–240. [in Russian]

1 INTRODUCTION

1.1 Background and actuality

An electrohydrodynamic (EHD) flow is a movement of liquid caused by the interaction between the electric field and the space charge that emerges in low-conducting liquid when the electric current passes through the bulk. Heightened interest to EHD flow is explained by the fact that it exemplifies the direct transformation of the electric field energy into the kinetic energy of fluid motion and that it plays an important role in the electric conductivity of dielectric liquids. Therefore, the investigation of EHD processes is of great significance for development and improvement of the physical model of processes of current passage through liquid dielectrics. EHD flows find wide application in modern knowledge-intensive technologies, and a number of applied EHD devices have been developed on their base. EHD pumps, heat exchangers, atomizers and filters are examples of such applied devices. They feature simplicity and compactness of design, the absence of moving and rubbing parts and high efficiency.

The first mention of EHD flows dates back to the early 18th century when the operations with high voltage became possible. At that time, F. Hauksbee made a report of ionic wind (i.e., EHD flow in the air), and, a century later, M. Faraday described EHD flow in liquid. However, the EHD flow came to be systematically investigated only in the middle of the 20th century. The number of research works and their scientific level have considerably increased during past decades, and the results of the investigations have essentially modified electrophysics and electrohydrodynamics of liquids, gases and plasma. EHD phenomena have been found to be observable everywhere—from the micro scale in cells of living creatures and liquid crystals up to the macro scale, e.g., in thunderstorm clouds. At present, the interest to electrohydrodynamics is high, and international conferences and symposia on the subject take place every year.

Electrohydrodynamics is based on the fundamental works on study of the electric conductivity of liquid dielectrics and EHD flows (Onsager, 1934; Plumley, 1941; Adamczewski, 1969; Felici, 1971; Bologa et al., 1977; Ostroumov, 1979; Stishkov and Ostapenko, 1989; Bartnikas, 1994; Castellanos, 1998). These books and papers comprise a huge amount of the experimental data (on characterization of liquid dielectrics properties, investigation of EHD flows, etc.) and theoretical research. The latter defines a whole

complex of processes that underlie electrohydrodynamics. Also, scientific view of electrophysics of liquid dielectrics and processes of electric current passage through their bulk is systematized and expanded in these books.

As the EHD and the physics of dielectric liquids at whole evolved, the main directions of investigations in this field of science were formed. They are the research of charge formation mechanisms and processes of current passage through low-conducting liquids, the investigation of EHD flows and breakdown strength, the development of experimental methods for diagnostics and property characterization of liquid dielectrics as well as the issue of application of EHD effects (liquid pumping, drop coagulation, electric atomization, intensification of heat exchange, spinning, filtration, etc.). These problems are closely interrelated, and a lag in the study of one part of them tends to retard progress of the others.

Possibility of using EHD flow both to practical purposes and as an object for fundamental research defines the topicality of the present work. Moreover, the need to develop efficient methods for computer-aided design of EHD devices with the view of improving their performance is acute due to the non-linearity of the set of governing equations and the unavailability of its analytical solution. Besides, it is worth noting that even the numerical calculations of EHD problems were so far performed only under simplified (sometimes, under oversimplified) statements due to high complexity of numerical computation schemes, strict criteria of getting convergent solutions and high demands for computing power. Recently, however, it became possible to conduct computer simulation of EHD problems in the complete approach based on the set of the Poisson, Navier–Stokes and Nernst–Planck equations owing to the development of programs for numerical calculation of partial differential equations and considerable growth of computing power.

With the beginning of active investigations of EHD flows with the help of computer simulation, the issue of prevailing mechanism of charge formation that leads to emergence of space charge density in the bulk (Apfelbaum and Yantovsy, 1977; Ostroumov, 1979; Stishkov and Ostapenko, 1989; Pankratieva and Polyansky, 2006) became more topical. Whereas one or another mechanism was used earlier only to explain and interpret the experimental data, the conduction of computer simulation necessitates the introduction of the formation mechanism into the computer model explicitly (into either the equations or boundary conditions). In the opinion of some researchers (e.g., Atten, 1974; Tobazeon, 1984; Stishkov, 1986), the prevailing mechanism is the so-called injection, i.e., the space charge formation at the liquid–metal interface. At the same time, other researchers believe that it is the intensification of dissociation rate under the influence of temperature (e.g., Ostroumov, 1979) or the electric field strength (e.g., Apfelbaum and Yantovsy, 1977), i.e. the Wien effect (Onsager, 1934; Frenkel 1938; Plumley, 1941; McIlroy and Mason, 1976) that leads to the emergence of EHD flow. Furthermore, there is another type of EHD flow that is directed oppositely, i.e., towards the sharper electrode (Jeong and Seyed-Yagoobi, 2002; Feng and Seyed-Yagoobi 2007).

Such contradictions and an insufficient level of knowledge of the issue of the prevailing mechanism of charge formation leading to the emergence of EHD flow also substantiate the topicality of the conducted PhD research. Moreover, performing computer (numerical) experiments that let one investigate the features of EHD flow structure under both mechanisms of charge formation plays a particular role in getting the issue resolved.

1.2 Previous and related studies.

1.2.1 Governing equations and the simulation technique.

The classical set of governing equations (Felici, 1971; Gogosov and Polyansky, 1976; Ostroumov, 1979; Castellanos, 1998) describing the EHD processes in liquid dielectrics contains three modules—the electrostatics module, the hydrodynamics module, and the charge transport one. These three modules correspond to the Poisson, Navier–Stokes and Nernst–Planck equations, respectively. Unlike the classical hydrodynamics where two main problems (flows around different bodies and flows in pipes) are considered and where fluid movement is caused by pressure gradient and the external force is absent, EHD flow has a speciality due to the presence of bulk force. This bulk force is the Coulomb one. Although it fails to act upon the entire bulk, but only upon ions whose concentration is many times less than that of neutral molecules, the representation of the bulk force as the product of the space charge density and the electric field strength is justified due to the following reasons. Firstly, the mechanical momentum in a fluid is efficiently transported from the "ionic grid" to neutral molecules due to the viscous interaction as it was shown by Stishkov and Samusenko (2010). Secondly, such approach is generally accepted in EHD (Felici, 1971; Ostroumov, 1979; Melcher, 1981; Castellanos, 1998).

The EHD equations are non-linear and have a strong interdependence, and unknown quantities are time-dependent. This all preconditions the complication of numerical calculations of EHD processes. Moreover, to make computer simulation of EHD flows, it is necessary to resolve a number of difficulties. They are the mathematical description of charge formation processes, the definition of closed equation set to describe the problem under consideration with necessary completeness, the specification of boundary conditions, the choice of method for numerical calculation and the technique for its stabilization, etc.

In view of the above, the main progress in the simulating EHD processes began only in this century. Earlier calculations (e.g., Perez and Castellanos, 1989; Perez et al., 1995) were concerned mainly the appraisal of the role of separate parameters, the definition of specific non-dimensional variables and computations of hydrostatic cases. Because of complexity of the EHD equation set, various simplifications were employed to solve it, and a number of researchers developed both algorithms and programs for the numerical integration of corresponding differential equations (Pankratieva and Polyansky, 1995; Higuera, 2000, 2002; Yazdani and Seyed-Yagoobi, 2010; Shelistov et al., 2012). However, using complete software packages has proved to be more perspective. Even though the latter failed to enable solving the problem in the complete approach, they nevertheless let one use complete algorithms for numerical solution of the equations. A number of works made in St. Petersburg State University are devoted to using simplified iterative algorithm for the computation of steady-state (Glushchenko and Stishkov, 2007; Stishkov et al., 2005, 2006; PI; AIV) and transient EHD flows (Stishkov and Elagin, 2005; Elagin and Stishkov, 2005; Stishkov et al., 2007) in finite-element software package ANSYS®. Afterwards, similar method was sometimes resorted to in works of researchers abroad (e.g., Lastow and Balachandran, 2006).

There are several alternatives for solving EHD problems. Two of them are the particle-in-cell method and the flux corrected transport one. As shown in work by Vazquez

et al. (2006), the results obtained using these methods are in a good agreement among themselves. The main advantage of these methods is a very high stability of numerical schemes when solving equations of the hyperbolic type even in the presence of steep gradients. The particle-in-cell method was developed for plasma simulation, and the flux corrected transport one—for calculating shock waves. A number of computations of the complete set of EHD equations both in 2D (Vazquez et al., 2006, 2008a,b) and 3D cases (Vazquez et al., 2011) were performed using these methods supplemented with the finite element one for calculation of the Poisson and Navier–Stokes equations. Beside some advantages, these methods require very high computing power and, moreover, have clouded prospects for calculating EHD problems at non-zero level of low-voltage conductivity. It is noteworthy that the computer simulation in mentioned works was conducted in the simplest geometry, but then it made it possible to perform computations in non-dimensional form.

Another approach to the computer simulation of electroconvection is based on the finite volume method (FVM) with different algorithms of discretization, letting one obtain a stable solution at a realistic value of diffusion. Examples of using the FVM for EHD problems can be found in a series of papers by Koulova et al. (2008), Perez et al. (2008), Traoré et al. (2010), Traoré and Pérez (2012). In these papers as in the ones described above, the simplest geometries are used (which lets authors make non-dimensionalization of the equations), the case of constant injection is considered, and the dissociation charge formation is excluded from examination. The latter approximation strictly bounds the scope of applicability of the approach for calculating EHD flows in liquids with considerable contribution of low-voltage conductivity to the total current. Besides, the FVM is unsuitable for solving problems with the axial symmetry in 2D axisymmetrical statement.

Finally, the method employed in the present study is based on the finite element method (Zienkiewicz et al., 2005). The issue of steep gradients and poor convergence of the solution is settled using the slightly exaggerated value of the diffusion coefficient, which has yet no effect on the results of computations (PII). As in previous cases, the complete set of EHD equations is used in the method. Examples of applying the method to calculations of EHD problems can be found in (Elagin and Stishkov, 2009; Stishkov and Elagin, 2009; Ashikhmin and Stishkov, 2012a; AIII). It is worth noting that the method lets one take into account the dissociation charge formation in the bulk including the Wien effect (AIII; AVII; PII) and conduct simulation of applied electrophysical devices with actual geometry (Ashikhmin and Stishkov, 2012b,c; AXII; AXIII). The method is realized on the base of commercial software package COMSOL Multiphysics®, which uses efficient and robust numerical schemes for solving sets of differential equations.

1.2.2 The experimental technique

Experimental investigation of the EHD flow structure is conducted using particle image velocimetry that is widespread in classical hydrodynamics (e.g., Van Dyke, 1982). Unlike the latter, visualization of the EHD flows is linked with a number of difficulties since there is a strong electric field in the experimental cell, which may cause self-contained movement of seeding particles relative to the liquid. Aluminum particles were used for flow visualization in early works, and at present, the preference is given to SiO_2 particles (Daaboul et al., 2009) or air bubbles (Afanasyev et al., 2007; Stishkov and Ostapenko,

1989). Besides, the latter have the advantages that they actually have no effect on electrophysical properties of a liquid and remain uncharged, and the electric field has no effect on them, which was investigated, in particular, by Lewin et al. (2008).

After the performing the flow visualization, computer image processing of experimental video frames is used to obtain quantitative data. At present, there are several basic methods to recover the velocity field of an EHD flow using seeding particles with the Particle Image Velocimetry (PIV) and the Particle Tracking Velocimetry (PTV) (Raffel et al., 2007) being the most common. The difference between them is as follows. The density of seeding particles is low in the PTV method, and it lets one track the movement of separate particles between consecutive frames. Corresponding results can be found, e.g., in works by Buyanov and Stishkov (2003, 2004) and Stishkov and Ostapenko (1989). As compared to the PTV method, the density of seeding particles in the PIV method is much higher, and tracking an individual particle between frames is very complicated; however, a standard statistical analysis can be applied. The examples of using the PIV method to obtain the velocity field of EHD flow can be found in works by Daaboul et al. (2008, 2009). It is worth noting that the PTV method can, as distinct from the PIV one, be used in the case of highly non-uniform velocity distribution since it lets one recover the entire trajectories of separate particles and provide for their manual processing if necessary (AVIII).

1.2.3 General investigation of EHD processes

The study of EHD flows can be conventionally divided into two groups by the symmetry of the electrode system. Symmetrical systems like plane–plane are the most convenient both for experimental research and for theoretical description, therefore, a number of investigations is conducted for them (Schneider and Watson, 1970; Watson et al., 1970; Hopfinger and Grosse, 1971; Atten, 1974; Traoré et al., 2005; Koulova et al., 2008; Kourmatzis and Shrimpton, 2012). A feature of the systems is that the EHD flows in them are similar to thermo-convective Bernard cells. In addition, the flow turbulization takes place in the transient regime after the pulsed application of the voltage as it was shown in experimental research (Hopfinger and Grosse, 1971) based on the schlieren method and, in the sequel, in the computer simulation (Kourmatzis and Shrimpton, 2012). Symmetrical electrode systems can also be of wire–wire (needle–needle) type. They are of special interest for studying the recombination of oppositely charged jets (Elagin and Stishkov, 2005) and the features of deceleration area in the absence the electrode at the point of the collision of two jets (Buyanov and Stishkov, 2003; AVI) as well as for practical application (Ashikhmin and Stishkov, 2009, 2012c; Buyanov and Stishkov, 2004).

In turn, heightened interest to non-symmetrical electrode systems is displayed since the highly non-uniform electric field distribution can be obtained there, which considerably enhances the near-electrode processes of charge formation even at relatively low voltage across the interelectrode gap. Initially, such systems were investigated experimentally (e.g., Stishkov and Ostapenko, 1989; Stuetzer, 1959), and a number of applied devices (e.g., EHD pumps, atomizers, etc.) were created on their base (Shrimpton, 2009b). Besides, the interest to them has grown recently (Daaboul et al., 2008; Louste et al., 2008; Traoré et al., 2010) due to improvements of experimental methods and the reduction of tiresome work on data processing (as a result of using PIV method).

It is the systems with highly non-uniform electric field distribution, which have become the focus of most part of works on computer simulation, since theoretical research for them is complicated. These works investigate basic features of hydrodynamic flows with the bulk force (Lazarev and Stishkov, 2006), conduct the comparison of EHD flows in liquids with those in gases (Stishkov and Samusenko, 2010) and with natural convection (Perez et al., 1995; Castellanos, 1998; Stishkov and Elagin, 2009), specify the flow kinematic structure (Stishkov et al., 2005; Elagin and Stishkov, 2009; PI), and provide description of the force one (AVI; AXI). Besides, some papers concern comparison of the computer simulation results with the experimental data, showing good agreement between them (Stishkov et al., 2005; Glushchenko and Stishkov, 2007; Traoré et al., 2010; PI; AIII), and also provide the estimation of the magnitude of space charge density (Traoré et al., 2010; AIV), which is very difficult to obtain directly in experiments with rare exceptions (Stishkov and Baranovsky, 1983; Tobazeon, 1984).

Accumulation of a large amount of experimental data and computer simulation results promoted improvement of physical model of EHD phenomena and stimulated carrying out theoretical research. In this light, two modern review papers (Denat, 2011; Zhakin, 2012) that generalize results of a number of investigations are of special interest. Another review paper (Grosu et al., 2007) considers various models of liquid charging and corresponding distributions of the electric field strength and gives their mathematical descriptions. In addition to analytical results, some data on the numerical computation of current passage processes in low-conducting media are also presented in this paper.

Another important issue is the role of EHD flow in the electrical conductivity of liquid dielectrics. Thus, papers (Stishkov and Ostapenko, 1979b; Tobazeon, 1984; Higuera, 2002) state that the high-voltage section of a current–voltage characteristic (CVC) is explained by the emergence of EHD flows, and paper (Stishkov and Ostapenko, 1979b) shows the increase of conductivity to begin immediately after the onset threshold of EHD flows and to continue as their intensity increases. Yet, a number of papers concerning CVC of liquid dielectrics (e.g., Polyansky and Pankratieva 1999; Apfelbaum and Apfelbaum, 2001; Zhakin, 2003; Denat, 2011) investigates only mechanisms of charge formation or dependence of the electric conductivity on the electric field strength, but disregards electroconvection. Substantiation and scope of applicability of the former and the latter approaches have been open to question for a long time due to complexity of processes under examination. However, it became possible to perform calculation of current passage processes on the base of the complete set of EHD equations, i.e., consider convective and migration mechanisms of charge transport jointly, owing to development of computer simulation software. It allowed one (in a few instances) to study interrelation between mechanisms of charge transport and define the contribution of each to the total current value (PII; PIV; AV). Besides, it is worth noting that a similar issue of the effect of the low-voltage conductivity value on the EHD flow intensity (and, thereby, on their role in the current passage) and on the non-linearity of CVC was considered earlier in the experimental work (Stishkov and Ostapenko, 1979a).

1.3 Present contributions

The goal of the present work is to provide comprehensive investigation of EHD flows in low-conducting liquids and reveal features of their kinematic, force and electric current structure under the injection and dissociation mechanisms of charge formation.

The object of research is liquid dielectrics with low-voltage conductivity in the range from 10^{-13} to 10^{-7} S/m (on the base of transformer and petrolatum oils).

Scientific novelty of the obtained results is as follows:

- A new method has been proposed for computer simulation of EHD flows and calculation of the integral current characteristics, which lets one take into account both the surface and bulk space charge formation and the dependence of the dissociation rate on the electric field strength;
- First ever analysis of the transient mode of the EHD flow formation after pulsed voltage application under the injection and dissociation mechanisms of charge formation has been conducted and instabilities of EHD flows that take place in the case of the strong injection have been explained;
- For the first time, the kinematic and charge structure of EHD flow in the case of charge injection into liquid with finite (non-zero) conductivity has been numerically calculated, and a change of the polarity of near-electrode layer, when the injection current density begins to prevail over the conduction one, has been shown to take place with the direction of EHD flow being reversed;
- For the first time, the energy transformation and the force structure have been analyzed, and on the basis of it, explanation of the specific zone structure of EHD flows revealed earlier in the experiments has been given;
- For the first time, current-voltage and current-time characteristics have been obtained in numerical calculations with taking into account both the convective and migration mechanisms of charge transport and the Wien effect occurrence.

The theoretical significance of the present work is as follows. The results of computer simulation and their comparison with the experimental data improve the physical model of EHD flows and, thereby, significantly contribute to the study of the issue of the electric conductivity of liquid dielectrics. The practical value consists in that the proposed method of computer simulation is applicable to calculation of EHD flows in low-conducting liquids with non-zero level of low-voltage conductivity and can be utilized for computer-aided design of applied EHD devices and their optimization. The performed numerical experiments clarify the role of the injection and dissociation mechanisms in the emergence of EHD flows and allow conducting more profound analysis of the experimental data. Calculated integral current characteristics explain part of the data on dynamic current–voltage characteristics presented in the literature.

A feature of the methodology of the present research is the application of integrated approach based on the unity of the computer simulation and the experimental investigation of EHD processes. The geometry of computer model closely corresponds to that of the experimental cell. The numerical calculation of the set of equations bases on the time-domain finite element method. The particle-tracking velocimetry method is used to experimentally obtain the velocity field of EHD flow.

The following confirms the dependability of the obtained results:

- use of proven methods for numerical calculations and trusted commercial software;
- high quality of the finite element grid and the application of adaptive time step when solving time-dependent tasks;
- a posteriori verification of the laws of conservation of energy and charge after the completion of the solution;
- comparison of results obtained in the experiment and in the simulation;
- use of precision measuring instruments, reliable experimental techniques and computer processing of the experimental data.

1.4 Appraisal of the work

The results of this work were presented at following conferences and symposia: IEEE International Conference on Dielectric Liquids (Poitiers, France – 2008 and Trondheim, Norway – 2011), International Symposium on Electrohydrodynamics (Sarawak, Malaysia – 2009 and Gdańsk, Poland – 2012), International Conference on Electrostatics (Budapest, Hungary – 2013), Symposium "Electrical Methods of Material Treatment" (Chişinău, Moldova – 2010), International Conference "Modern Problems of Electrophysics and Electrohydrodynamics of Liquids" (St. Petersburg, Russia – 2006, 2009, and 2012), International Scientific-Practical Conference "Basic and Applied Researches, Development and Application of High Technologies in Industry and Economy" (St. Petersburg, Russia – 2010 and 2012), International Conference "Models and Methods in Aerodynamics" (Yevpatoriya, Ukraine – 2010), Plyos International Conference on Nanodispersed Magnetic Fluids (Plyos, Russia – 2008), Russian Conference "Physicochemical and Applied Problems of Magnetic Dispersed Nanosystems" (Stavropol, Russia – 2011).

The results of this work were published in 20 papers (6 in Web of Science and Scopus database). The main content of this work can be found in the included articles PI–PIV.

2 MAIN PART

The computer simulation and the experimental investigation with subsequent computer processing of the experimental data are the main tools in the present work. Therefore, first, descriptions of utilized methods, the geometry of the system, fluid properties, and parameters of equipment are given below. Then, the results of computer simulation of EHD flows and calculation of the integral current characteristics and some experimental results are presented. Finally, main achievements are listed and conclusions are formulated.

2.1 The simulation technique

2.1.1 Governing equations

The simulation base is the complete set of EHD equations, describing the current passage processes in isothermal incompressible liquid dielectrics. Consider its features only, since all corresponding equations and decision variable are specified in the included article PII.

The space charge density distribution that defines the acting force area of the flow and, thus, plays the key role in EHD is calculated on the base of the Nernst–Plank equation. The corresponding distribution is dependent on both the charge transport and charge formation mechanisms. The latter means the process that leads to the emergence of ions in a dielectric liquid. It can be either the dissociation of molecules in the bulk (which leads to formation of at least two ion species) or the so-called injection that is linked with the electron exchange between metal and molecules of a liquid. In the latter case, ions of one species with the same polarity as the active electrode emerge. It is worth noting that the obtained space charge density distribution appears in the Poisson equation directly, which lets one calculate the electric field strength taking into account the space charge influence on it. In its turn, this enables one to compute EHD flows in the case of strong injection when the formed space charge considerably decreases the electric field strength near the active electrode and, thereby, lessens the intensity of space charge formation.

The mechanism of charge formation is taken into account in simulation directly. In the injection model of charge formation, the source function g_i in the Nernst–Planck equation is set to zero in the case of unipolar injection and is equal to the recombination term (that is described below) in the case of bipolar one. The functional dependence of the

injection current density on local electric field strength $j_{\mathrm{inj},i}(E)$ and the condition of charge loss j_{loss} is set at the surface of every electrode:

$$j_{\mathrm{inj},i}(E) = f_i(E) \tag{1}$$

$$j_{\mathrm{loss}} = d_i(n, E). \tag{2}$$

The theoretical determination of functional dependence $f_i(E)$ is a very intricate issue that requires taking into account kinetic reactions occurring at the metal–liquid interface. At present, even very complicated theories (Zhakin, 2006) dealing with electrochemical reactions at the electrode surface fail to explain all variety of the observable results. Moreover, the formulation of universal boundary conditions for the charge transport equation is impossible since various physicochemical processes can occur under high voltage depending on the properties of electrode surface and liquid (Zhakin, 2012).

In spite of complexity of near-electrode reactions, introducing a phenomenological function dependence of injection on the local electric field strength lets one advance in a simulation and obtain satisfactory results. Thus, the dependence of the Fowler–Nordheim equation kind is used in the present work:

$$f_i(E) = A_i \exp(-B_i/E). \tag{3}$$

Application of the exact Fowler–Nordheim dependence used to arouse criticism since it fails to provide enough current density under realistic conditions. Nevertheless, paper (Zhakin et al., 2012) shows the possibility of the emergence of field electron emission when taking into account the real nanostructure of the metal surface and introducing electron-acceptor impurities into the liquid. Function (3) has a simple form—it is almost linear in the characteristic (for EHD) range of the electric field strength and is close to zero under the voltage below the threshold of EHD flow onset. Besides, fitting coefficients in (3) has allowed us to achieve satisfactory agreement between the experimental and computer simulation results, which is shown, in particular, in paper (AIII). The values of coefficients A and B depend on the properties of the electrode metal and of the liquid and may vary in a certain interval. Therefore, A and B in the present work are treated as the parameters of analysis that determine the intensity of injection.

The charge loss at the electrode surface is a retroaction with the injection that leads to the ion neutralization by means of the transition of excess electron to the anode or the reduction of electron from cathode. Function $d_i(n, E)$ describing the charge loss is typically set proportional to the ion concentration in the near-electrode area. One of the alternatives of the loss condition is to set the function $d_i(n, E)$ equal to the total current density for ions arriving to the boundary from the bulk:

$$d_i(n, E) = j_{\mathrm{bulk},N}, \tag{4}$$

$$\vec{j}_{\mathrm{bulk}} = n_i b_i \vec{E} - D_i \nabla n_i, \tag{5}$$

where subscript N denotes the normal to the surface of the electrode. Condition (4) means that the neutralization of ions occurs instantaneously as soon as they touch the electrode, i.e., the electrode is “transparent” for the ion flux.

Now consider the dissociation model of charge formation. It assumes that ion formation takes place in the result of dissociation of molecules, and at that, not the ones of dielectric liquid itself but those of impurities dissolved in it. The reaction of dissociation proceeds above all due to the energy of thermal molecular motion, and therefore, the

mechanism operates even without the external electric field. The recombination reaction occurs in the bulk simultaneously with the dissociation one, its intensity being proportional to the product of concentrations of oppositely charged ions.

The bulk source of the ion creation (dissociation) and the term describing their loss (recombination) is introduced into the right-hand side of the Nernst–Planck equation in this model as distinct from the injection one. It is noteworthy that the ion loss takes place not only due to recombination, but also at the surface of the oppositely charged electrode as it is in the injection model.

The intensity of dissociation in the presence of a strong external electric field increases exponentially (Castellanos, 1998; Zhakin, 2003), which is known as the Wien effect. The dissociation rate in non-polar liquids (at $\varepsilon \approx 2$) rises nearly twice under the effect of a relatively weak electric field (about 10^6 V/m) and about 40 times under that of a stronger one (about 10^7 V/m) (Zhakin, 2003). The dependence of the relative increase in the dissociation rate on the local electric field strength $F(p)$ was derived in the theory of ion pairs and has the following asymptotic form:

$$F(p)(E \to \infty) \approx \frac{\exp(4p-2)}{2p} \tag{6}$$

$$p = \frac{e}{2k_B T}\sqrt{eE/(4\pi\varepsilon\varepsilon_0)}. \tag{7}$$

The relative increase in the dissociation rate in a more complicated model introduced by Onsager (1934) is expressed via the Bessel function:

$$F^{\mathrm{Onz}}(p) = \frac{I_1(4p)}{2p}, \tag{8}$$

where I_1 is the modified Bessel function of the first kind.

2.1.2 Features of the simulation technique

A possibility to solve the complete set of EHD equations appeared comparatively recently due to its complexity, so some results of the present work were obtained on the base of the simplified approach (PI; AIV). The latter disregards migration and diffusive charge transport since the fluid velocity is many times the ion drift one in the most part of the interelectrode gap (Stishkov and Ostapenko, 1989) and only two moduli—the Navier–Stokes equation and the Poisson one—are calculated. This algorithm is not a self-sustaining one since using it requires the radius of charged jet to be set a priori, which, in turn, calls for carrying out a preliminary experiment.

However, such approach lets one conduct calculations and the analysis of steady-state EHD flows in the injection model of charge formation in spite of a number of simplifications. Thus, on the base of the comparison of the computer simulation results (obtained using this method) and the appropriate experimental data, the magnitude of the space charge density in the central jet of EHD flow was estimated (PI; AIV), which was practically impossible to realize directly in the experiment. In addition, the comparison of the EHD flow structures in the needle–plane and needle–needle electrode systems was made and distributions of force density along fluid flow lines were analyzed on the base of the simplified approach (AVI).

The complete approach, presented in detail in (PII; PIV), presupposes the computation of the complete set of EHD equations. Moreover, the time-dependent problem is considered directly, making it possible to study and analyze both the processes

of EHD flow formation and the steady-state distributions. The numerical computations of the set of equations are performed using software COMSOL Multiphysics®, which is very convenient and promising for simulation of EHD problems. Its main advantages are as follows:

- the possibility to solve jointly several types of equations (in our case—the Nernst–Plank, Navier–Stokes and Poisson ones);
- all equations are explicitly shown and every parameters in them is changeable;
- the comparative simplicity of the model construction and setting the necessary conditions;
- the availability of a direct solver that enables to solve problems fast;
- the easy-to-use algorithm of the load specification.

The main disadvantage of the chosen software is the high requirements to the computer power and especially to the main memory capacity.

Using the finite element method that underlies the computations in COMSOL Multiphysics®, in particular, means that all decision variables are described in the continuum approximation (unlike, e.g., the particle-in-cell method that is also used to solve EHD problems). Nevertheless, such approach is justified in spite of discontinuity of ion distribution. Firstly, it is generally accepted in EHD, and secondly, simple estimation show that the considerable amount of ions corresponds to every finite element. Thus, there are about one hundred of ions even in a rather small finite element of 10 μm linear dimension (e.g., in near-electrode area) at the space charge density of 0.01 C/m^3 (that is a typical one for an EHD flow).

2.1.3 Geometry of the computer model

As mentioned above, the injection and especially the Wien effect take place under a strong electric field (about 10^7–10^8 V/m); therefore, to study them, it is convenient to use electrode systems with highly non-uniform electric field distribution, e.g., wire– or needle–plane. In such systems, the local electric field strength in near-electrode area is many times its average, which enables studying charge formation mechanisms even at low voltage across the interelectrode gap to avoid the electrical breakdown of liquid.

The major part of the present research is carried out for the needle–plane electrode system. The interelectrode gap in the computer model is the same as that in the experimental cell and amounts to 7 mm. This length was chosen taking into account the results obtained in the investigation of the influence of the gap length on the EHD flow structure (Stishkov et al., 2006). Thus, according to the latter, there is no overlap of acceleration and deceleration zones and the fluid velocity decreases insignificantly along the model axis at the chosen gap length. The consideration of 2D axisymmetric model is sufficient to simulate the needle–plane system since the latter has the axial symmetry (excepting the case of turbulent flow that violates the symmetry).

The geometry of the computer model and boundary conditions for the set of equations are presented in Fig. 1. The degree of non-uniformity of the electric field distribution, i.e., the ratio of its maximum intensity to the average value, is about 50.

Since the high-voltage charge formation is dependent on the local electric field strength, then, to improve the conformity between the computer and experimental models,

the needle shape in simulation was constructed using splines that approximate the shape of the experimental needle as photographed by digital camera with microscope.

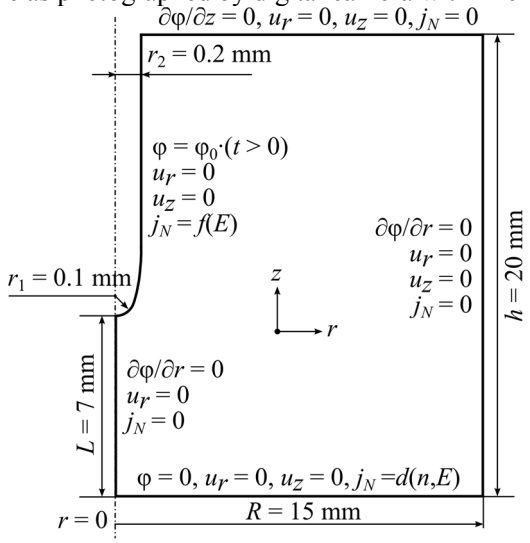

FIGURE 1 Geometry of the computer model and boundary conditions for the set of equations.

The liquid properties correspond to those of transformer oil: $\varepsilon = 2.2$, $\gamma = 870$ kg/m^3, $\eta = 0.025$ Pa s, $|b| = 10^{-8}$ m^2/V s (which is assumed to be the same for ions of both polarities), and $|Z| = 1$. The diffusion coefficient of monovalent ions according to the Einstein relation is $D = 2.5 \cdot 10^{-10}$ m^2/s; however, exaggerated value $D = 10^{-7}$ m^2/s is used in the simulation for better convergence, which nevertheless has no effect on the results of computations (PII). Low-voltage conductivity σ_0 is a parameter of study, and its value is varied with other properties of the liquid left unchanged. This paper considers the conductivity values in the range from 10^{-12} to 10^{-8} S/m. As will be shown, the range is of special interest because of a rapid growth of the role of the dissociation charge formation mechanism as compared to the injection one. In the injection model, the low-voltage conductivity is assumed to be zero.

2.2 The experimental technique

The experimental study of EHD flows offers a challenging problem, with the presence of a strong electric field (about 10 kV/cm) in the experimental cell being one of the main difficulties. Besides, the fluid velocity distribution is far from uniform. All this imposes a number of constraints on instruments and investigation methods to be used. Therefore, it is necessary to choose the most appropriate method for the EHD flow visualization with further computer processing and implement it in the experiment. The three-dimensionality of EHD flow in the case of the needle–plane electrode system is an additional complication that considerably raises demands to prospective methods for flow visualization and processing.

Small air bubbles introduced into the liquid through a special capillary were used as visualization particles (Stishkov and Ostapenko, 1989). The investigation of air bubbles

behavior showed that they has no effect on the low-voltage conductivity of liquid and the relative error in the measurement of EHD flow velocity, which is conditional on their individual motion, was within 5–10 % when using air bubbles with 10–50 μm in diameter. Visualization particles of this kind remain uncharged even under the action of strong local electric field that is a feature of electrode systems the needle–plane type, and so they remain unaffected by the Coulomb force. Theoretical study of the effect of dielectrophoretic force on bubble motion and corresponding experimental investigation is presented, e.g., in paper by Lewin et al. (2008). In view of the above, EHD flow is believed to be the major cause of bubble motion, which enables using these visualization particles to measure the fluid velocity.

As shown in the review of previous and related studies, the PIV and PTV (Raffel et al., 2007) are two most widespread methods for recovering the velocity of hydrodynamic flows by the motion of seeding particles. The methods differ in that the former implies processing of separate particle trajectories while the latter is based on the cross-correlation analysis of two consecutive video frames, which allows one to define the average velocity in separate sectors containing a great number of seeding particles.

Application of the PIV method demands very high quality of video capturing and processing, which, in turn, requires using expensive instrumentation. Besides, a large quantity of visualization particles is needed, which can lead to changes in liquid properties. In addition, the reliable processing of highly non-uniform flows seems to be rather complicated in view of the necessity to divide every frame into areas, within which fluid velocity should be approximately equal. Thus, the PTV method was utilized in the present work.

The trajectory of each seeding particle is tracked separately when using the PTV method. Thus, the particle trace is found on several consequent video frames, and then determined coordinates with corresponding time points are recorded into a matrix. As a result, set of points $\vec{x}_i(t_i)$ belonging to the same trajectory is obtained, which allows its approximation with a smooth curve. Such postprocessing improves the accuracy of the results and, moreover, yields the velocity values throughout the trajectory instead of isolated points.

To summarize, the PTV method has following advantages:

1) small amount of seeding particles is enough for the flow visualization and processing, and therefore, they leave properties of liquid unchanged;
2) owning to tracing each particle in course of several frames, it is possible to use trajectory approximation, which considerably improves the accuracy of velocimetry;
3) since particle tracks can be specified and revised in the manual mode and there is no need to divide every frame into areas with equal velocity, even highly non-uniform flows can be processed;
4) there is an opportunity to exclude some tracks from the processed ones that move at an angle of the recording plane, which, due to the three-dimensionality of investigated flows, has a great significance for the reliability enhancement;
5) the time resolution can be improved on demand by use of stroboscopic lighting.

However, the PTV method has two disadvantages:

1) the capability to accumulate a big amount of the experimental data is quite restricted because of the considerable time cost of track processing;
2) only steady-state flows can be processed.

The experimental study of EHD flows was conducted using a special test bench that makes it possible to visualize electroconvective flows, conduct their video recording and measure CVCs. Recording of all data is carried out using the computer equipped with a video capture device and an analog-to-digital converter. Main units of the test bench are described below.

The experimental cell presents a cylindrical vessel of a transparent plastic with the needle–plane electrode system inside. To study liquids with different properties (in particular, liquids with and without special impurities), several cells of close geometry were produced. The main one, for which the comparison of the experimental and simulation data was made, has the following dimensions: the diameter of the needle base is 0.4 mm, the radius of the needle tip is 0.1 mm, the interelectrode gap length is 7 mm, and the vessel diameter and height are 40 and 30 mm, respectively. In the cover of the cell, there is a special orifice for the capillary used for introducing visualization bubbles into the liquid. The needle electrode is connected to the high-voltage terminal of power supply, and the plane one is earthed through a current meter.

The high-voltage module contains a power supply VIDN–30 providing voltage of both polarities in the range from 0 to 30 kV with maximal current value 200 μA and a digital-to-analog converter DT9804–EC–1 used to control the voltage.

The video recording unit includes a USB video camera EVS 746 (with 740×576 resolution and 25 Hz frequency) and a computer with special software for frame capture and processing.

The unit for electrical parameter measurement is composed of two analog-to-digital converters L-Card L–761 and E14–140, voltage divider, current meter and picoammeter Keithley 6485.

The behavior of EHD flows depends on properties of the working liquid, as well as on the type of metal of the active electrode. In the present research, transformer and petrolatum oils were used as working liquids and butyl alcohol and iodine—as special impurities; the needle electrode was made of steel. Special impurities were used to increase stability and intensity of EHD flows and to conduct investigation of the effect of low-voltage conductivity on the flow structure. Table 1 presents basic properties of utilized liquids.

Table 1. Basic properties of the utilized liquids.

Liquid type	Mass density, kg/m^3	Dynamic viscosity, Pa s	Low-voltage conductivity, S/m	Ion mobility, $m^2/V\ s$	Relative electric permittivity
Transformer oil	870±5	0.02	$1.2\pm0.1\cdot10^{-11}$	$1\cdot10^{-9}$	2.2
Petrolatum oil	880±5	0.123	$1.5\pm0.5\cdot10^{-13}$	$5\cdot10^{-10}$	2
Butyl alcohol	810±5	0.003	$5.0\pm0.1\cdot10^{-6}$	$5\cdot10^{-9}$	17.7

To process experimental video frames, original program *EHD reader* (Afanasyev et al., 2007; AVIII) implementing the PTV method was used. The program is completely written under *MATLAB*® environment, supplemented with a convenient graphical user interface, and composed of two main modules. The first one provides image loading and allows specifying particle traces, while the second one implements track fitting, calculates

the velocity field, and plots obtained distributions. Capabilities of *MATLAB*® Image Processing and Spline Toolbox are utilized.

The following plots are constructed on the base of the processed experimental data: 1) the vector field of velocity; 2) the surface plot of velocity; 3) the contour plot of velocity; 4) processed tracks; 5) the velocity along chosen track; 6) the velocity and acceleration along the linear user-defined path. All obtained data can be exported to an external file for further processing.

2.3 EHD flow structure

At present, the computer simulation of EHD flows has a number of advantages over the experimental research since the former enables one to acquire a considerably greater amount of data (in comparison with the latter), to obtain distributions of unknown quantities in the entire domain, to investigate both kinematic and dynamic structures, and to study in succession the effects of various factors on the EHD flow structure.

2.3.1 The injection into non-conducting liquid

To begin with, consider the behavior of EHD flows in the classical case of unipolar injection into non-conducting liquid when there is only one ion species and no recombination in the bulk. Such model is rather simple though it agrees well with some experimental data and is used for characterization of a number of EHD devices (Shrimpton, 2009b).

Results of computer simulation of EHD flows in cases of the so-called weak and strong injection (where the degree of the electric field screening at the active electrode under the influence of the injected charge is implied under the injection power) is presented in the included articles (PI; PII) and in (AIII; AVII). There is no difference between methods of computer simulation in these two cases since the effect of space charge density on the electric field strength is directly taken into account. The computation of EHD flows is performed until the steady-state regime is obtained. The calculation of the complete set of EHD equations results in getting bulk distribution of unknown quantities—the fluid velocity, the space charge density, the hydrodynamic pressure, the electric field strength, and the lines of fluid and ion flow.

The zone structure of EHD flows in a system with highly non-uniform electric field was described and explained on the basis of results of calculations. Initially, the structure was revealed in experimental research (Buyanov and Stishkov, 2003; Stishkov and Ostapenko, 1989) for electrode systems with two-dimensional symmetry like wire–plane and wire–wire. Later, a similar structure was obtained and partially refined in the wire–plane (Stishkov et al., 2005) and needle–plane (PI; AXI) electrode systems using a simplified computer model of EHD flow (Fig. 2*a*).

Near both electrodes, there is a layer where the fluid velocity nearly vanishes. This is the motionless (or boundary) zone. The next zone is that of intense acceleration where the main energy conversion from electrical energy to kinetic one takes place. The large part of the interelectrode gap is a zone of quasi-uniform flow. Lines of fluid flow are practically straight and parallel to each other in this zone. Finally, there is an intense deceleration zone at the end of the interelectrode gap.

Unlike the qualitative description, the detailed analysis of the zone structure and its interpretation on the basis of the distribution of acting forces and energy balance is feasible only when the complete set of EHD equations is considered. To compare, Fig. 2*b* presents the surface plot of the fluid acceleration projection onto the velocity direction (at a voltage of 10 kV), which shows the authentic zone structure with quantitative data. Thus, the acceleration zone begins slightly above the needle tip and runs on for about 1.5 mm. The intensity of acceleration is distributed highly non-uniformly within this area and the maximum value exceeds 100 m/s^2. The deceleration zone is similar to the acceleration one in length, but is wider, narrows at the bottom part, and the intensity of deceleration is distributed comparably uniformly. The motionless zone is more clear cut near the plane electrode where the deceleration zone is situated at several tenths of millimeter from the metal surface, while the thickness of the boundary zone near the needle tip is negligible.

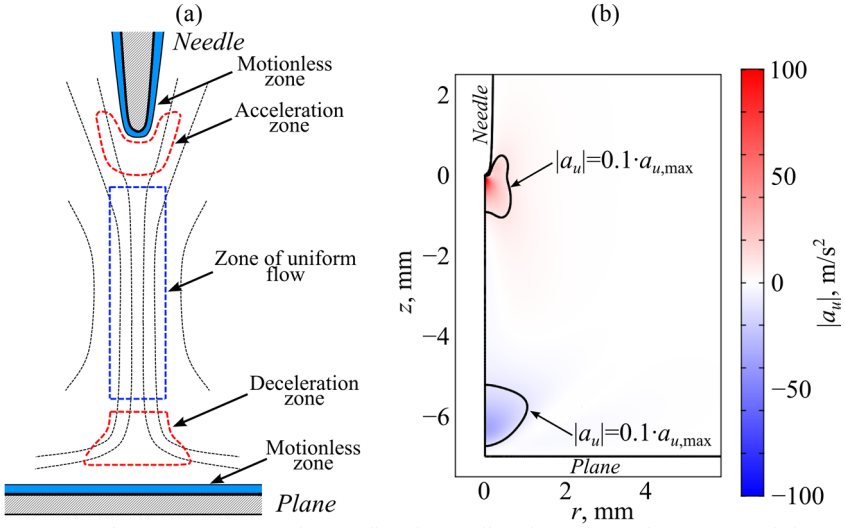

FIGURE 2 (a) The zone structure of EHD flow in needle–plane electrode system and (b) surface plot of the fluid acceleration projection onto the velocity direction.

To analyze the force density distribution and processes of energy conversion in the bulk of the cell, consider the time derivative of the total kinetic energy in the incompressible liquid (Landau and Lifshitz, 1987):

$$\frac{\partial}{\partial t}\frac{\gamma u^2}{2} = -div\left\{\vec{u}\left(\frac{\gamma u^2}{2}+P\right)-(\vec{u},\sigma')\right\}-\frac{1}{2\eta}{\sigma'}_{ik}{}^2+\rho(\vec{u},\vec{E}), \tag{9}$$

where ${\sigma'}_{ik}$ is the viscous stress tensor:

$${\sigma'}_{ik}=\eta\left(\frac{\partial u_i}{\partial x_k}+\frac{\partial u_k}{\partial x_i}\right). \tag{10}$$

The expression in the divergence operator in Eq. (9) represents the density of the energy flux inside liquid. The first term in curly brackets is the energy flux connected with a transfer of liquid mass under its motion, and the second one $(\vec{u},\sigma')$ is connected with the processes of internal friction. The latter is due to the fact that the presence of the viscosity leads to the emergence of momentum flux ${\sigma'}_{ik}$ associated with the energy transfer. The second term in the right-hand side of the equation corresponds to the density of dissipative power consumption, i.e., the irreversible energy loss due to the work of the friction force.

And the last term represents the density of power of changing fluid energy owning to the Coulomb force.

Proceeding from Eq. (9), it can be concluded that, in course of the fluid motion, the fluid energy is redistributed between, spent on, or got from the following:

- $\frac{\gamma u^2}{2}$ the density of the kinetic energy;
- P the density of the potential energy (that is immediately equivalent to the hydrodynamic pressure);
- A_{frict} the density of the work of the viscous force leading to dissipation;
- σ' the momentum flux between layers caused by the internal friction;
- A_{Coul} the density of work of the Coulomb force.

To provide more detailed analysis of the energy conversion, consider balances of forces and energy along a fluid flow line. The energy conservation law in this case is expressed in the following form:

$$\frac{\gamma u^2}{2} + P = \int_0^l (\vec{\mathcal{F}}_{\text{frict}} + \vec{\mathcal{F}}_{\text{Coul}}) d\vec{l} + const, \qquad (11)$$

which means that the sum of the kinetic and potential energy changes only due to the work of the Coulomb and viscous forces along a fluid flow line.

Consider the fluid flow line passing through the central jet of EHD flow in the close proximity to the model axis and, thus, inside the charged area (r_{min} = 0.15 mm). Fig. 3*a* presents the selected line depicted on the surface plot of fluid velocity.

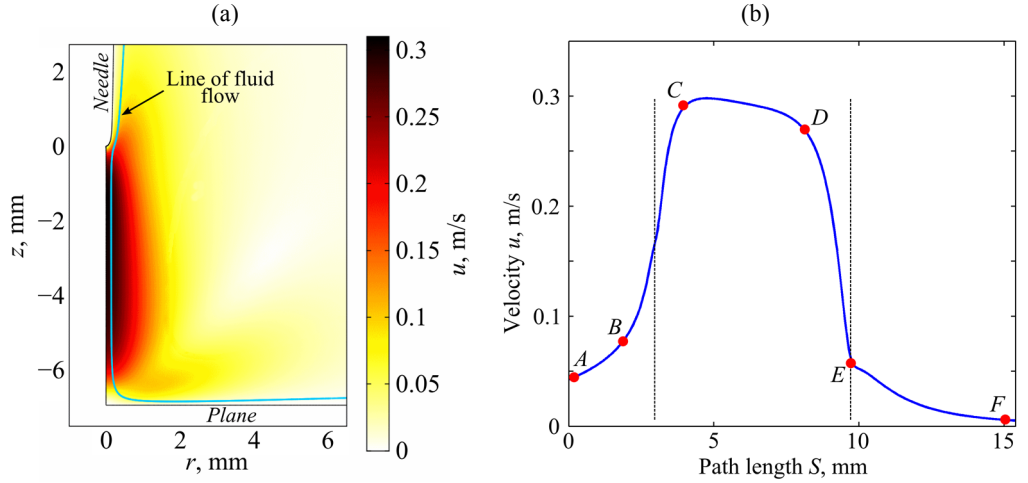

FIGURE 3 (a) The selected line of fluid flow depicted on the surface plot of fluid velocity and (b) the line plot of velocity distribution along corresponding path; vertical lines corresponds to the points of maximal approach of the line to the needle tip and to the center of plane electrode, respectively.

Fig. 3*b* gives the line plot of the velocity distribution along the major part (i.e., along the part shown in Fig. 3*a*) of the chosen fluid flow line. It is seen that the fluid starts to accelerate just above the needle tip (section "*A*–*B*" in Fig. 3*b*). Further on, the swift acceleration ("*B*–*C*"), the zone of quasi-uniform flow ("*C*–*D*"), and sharp deceleration

("*D–E*") follow in succession, and then smooth deceleration ("*E–F*") takes place after the knee of the curve ("*E*").

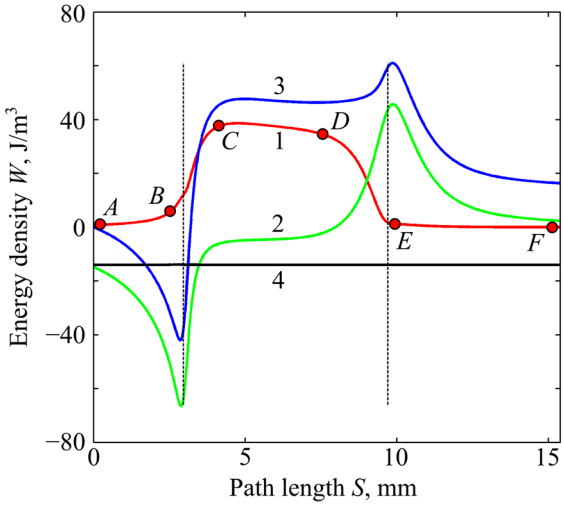

FIGURE 4 Distributions of the densities of energy and the integral of the total work of forces along the selected line of fluid flow: 1 and 2—the densities of the kinetic and potential energies, respectively, 3—the integral of the total work of Coulomb and viscous forces, 4—the difference between the total energy and the integral of the total work.

To explain the resultant velocity distribution, it is necessary to consider energy balance (Fig. 4). In the area above the needle tip (section "*A–B*"), the increase of the kinetic energy is caused by a decrease of the potential one, however this increase is small since most energy is spent on the work of viscous force. The growth of both the kinetic and potential energies at relatively short section "*B–C*" takes place due to the positive work of the Coulomb force. Further on, both kinds of energy remain almost unchanged over a rather long interval ("*C–D*") since the energy loss due to the viscous friction is compensated with the positive work of the Coulomb force. Then, the sharp deceleration of liquid at section "*D–E*" is brought about by the energy conversion from the kinetic energy into the potential one. And, at last, the viscous force starts to prevail, leading to a decrease of the potential energy (section "*E–F*"). Reliability of the presented energy distribution is confirmed by the fact that the difference between the total energy and the work of Coulomb and viscous forces presented by black line at the plot (Fig. 4) is a constant. Similar analysis of acting force distributions can be found in (AVI; AXI).

Summarize the results of computer simulation obtained at various voltages and construct the plot of the dependence of EHD flow average velocity on the voltage and electric current (Fig. 5). As can be seen, the average velocity exhibits a linear dependence on the voltage across the interelectrode gap, which agrees with typical experimental data for systems with less degree of the electric field non-uniformity. In turn, the velocity is proportional to the square root of the current and, besides, dependent only on its integral value, while the coefficients of the injection function (3) have low significance (when obtaining the same value of the total current).

2.3.2 The injection into low-conducting liquid

Proceed with considering a more complete model that takes into account the injection and dissociation mechanisms of charge formation simultaneously, i.e., the case of the injection into low-conducting liquid. Such model closely corresponds to a realistic case and makes calculations possible both in low- and high-voltage ranges. Besides, it allows simulating EHD flows caused by the conduction phenomena (Jeong and Seyed-Yagoobi, 2002; Feng and Seyed-Yagoobi 2007) (i.e., before the threshold of the injection onset) and obtaining CVCs in a wide voltage range with an account of both the surface and bulk charge formations and also the migration and convective mechanisms of ion transport.

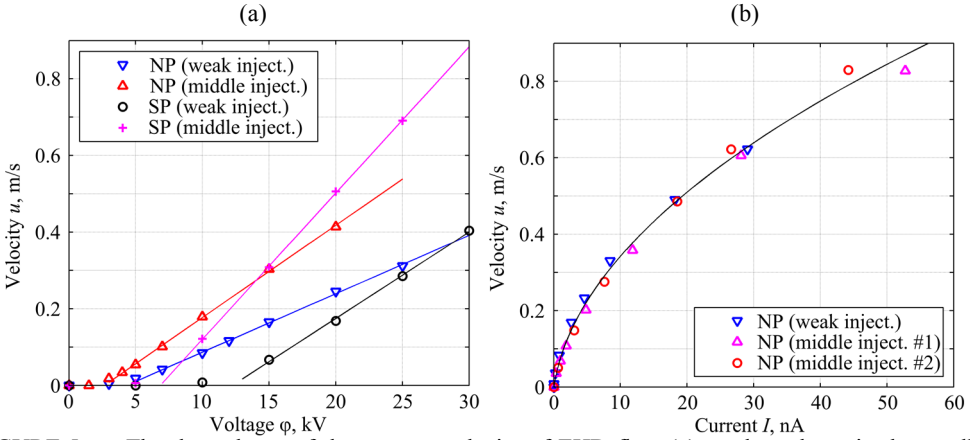

FIGURE 5 The dependence of the average velocity of EHD flow (a) on the voltage in the needle–plane (NP) and sphere–plane (SP) electrode systems (at weak and middle injection) and (b) on the total current value in the needle–plane system at various values of coefficients in Eq. (3).

To avoid excessive complication of the model, assume the unipolar ions originating as a result of both the injection and dissociation to exhibit the same behavior and for this reason confine our model to using only two different ion species.

The major results obtained in this model are presented in two articles (AI; AV) that show, in particular, how the reversal of the EHD flow direction and the polarity of near-electrode layer take place with the increasing voltage. Besides, these works analyze the influence of low-voltage conductivity value on the EHD flow structure. The latter result is of interest for the present work, and corresponding surface plots of the space charge density and fluid velocity distributions at a fixed voltage but at different low-voltage conductivity values are given in Fig. 6. They show how the ratio of the intensities of the surface and bulk charge formation influences the EHD flow behavior.

The EHD flow structure in the needle–plane electrode system remains practically unchanged (Fig. 6*a* and *d*) as the low-voltage conductivity increases from 0 up to 10^{-10} S/m and corresponds on the whole to the results for the model of injection into non-conducting liquid (PII; AIII). The charge injected into liquid arrives to the central jet from the entire lateral needle surface, while the non-equilibrium near-electrode layer is absent. The latter is caused by the fact that the injection current density considerably outweighs the conduction one coming from the opposite direction, which makes the recombination effect negligible. Nevertheless, the total conduction current can be of the same order of

magnitude or even greater than the total injection one (AV) since the latter runs only through the central jet while the former—throughout the entire bulk.

A jump in the charge structure of the central jet occurs with increasing the low-voltage conductivity value from 10^{-10} up to 10^{-9} S/m since the flux of ions originated due to the bulk dissociation starts to exceed the one of ions injected from the needle surface. Thus, the homocharge fails to penetrate inside the liquid from the entire lateral surface of needle but only from its bottom part at low-voltage conductivity $3 \cdot 10^{-10}$ S/m (Fig. 6*b*). And at higher conductivity level (10^{-9} S/m), ion penetration inside the liquid happens only at the needle tip with the reduced value of the space charge density.

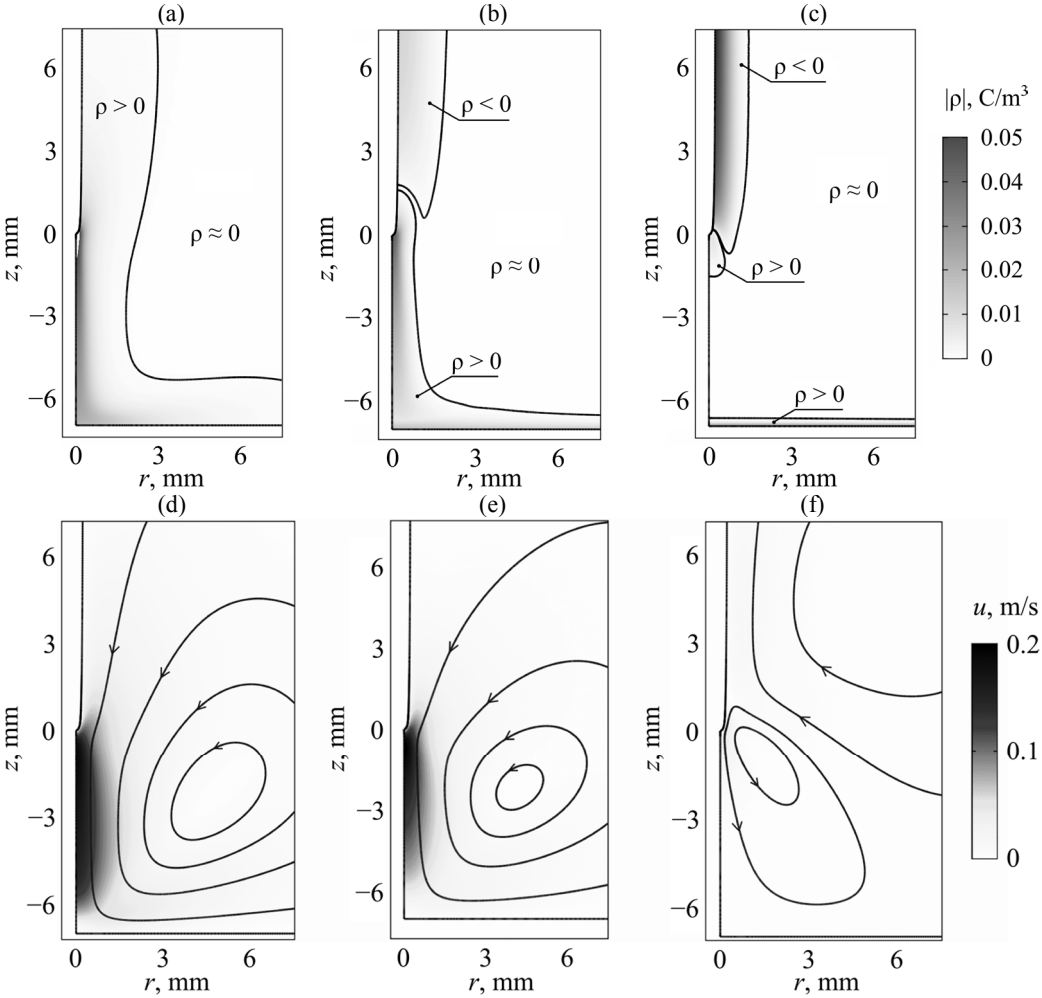

FIGURE 6 (a)–(c) The surface plots of space charge and (d)–(f) fluid velocity distributions and lines of fluid flow in the needle–plane electrode system at a voltage of 7 kV and at different levels of low-voltage conductivity: 0—(a) and (d), $3 \cdot 10^{-10}$—(b) and (e) and 10^{-9} S/m—(c) and (f); contour lines on the top plots correspond to the 0.01 level of the maximum of the space charge density.

To determine the cause of this feature, Fig. 7 presents two distributions along the needle surface: the injection current density and the current density needed to cover the ion

deficit in near-electrode area (at $\sigma_0 = 3 \cdot 10^{-10}$ S/m), which is equal to the part of the conduction current provided by ions of one polarity, i.e., $\sigma_0 E/2$.

This plot shows the injection current density to be less than the oncoming conduction current along the most part of needle surface, and therefore, there is no homocharge at the top part of the needle. The situation is vice versa at the bottom part of the electrode, and the ions being injected form a homocharge region near the needle tip while the heterocharge layer emerges above it (Fig. 6*b*). In this case, the central jet becomes narrower and the space charge density decays more rapidly. Hereupon, the decrease of EHD flow intensity takes place in this case, and lines of fluid flow depart from the axis below the acceleration zone (Fig. 6*e*). And at last, a limiting case is shown in Fig. 6*c* when the injected charge practically totally recombines and fails to penetrate inside the interelectrode gap, EHD flow becomes undeveloped and a return vortex (with the opposite direction of fluid flow) emerges (Fig. 6*f*).

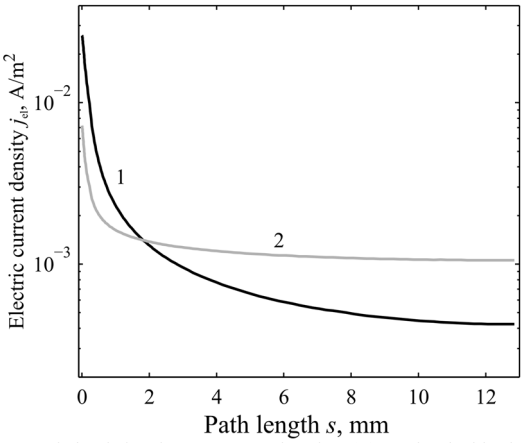

FIGURE 7 Distributions of the injection current density (1) and a half of the conduction one (2) (at $\sigma_0 = 3 \cdot 10^{-10}$ S/m) along the needle surface.

Thus, the low-voltage conductivity influences the EHD flow behavior in the following way. While the injection current density prevails over the conduction one, the space charge and velocity structures are in close correspondence to those obtained in the models without dissociation, and therefore the pure injection model of charge formation may be used in this range of the low-voltage conductivity. The only essential distinction between the models with and without taking dissociation into account is that the former one makes it possible to calculate a CVC in a more accurate way (especially, in the low-voltage range where the dissociation is the sole mechanism of charge formation). In turn, it gives one an additional opportunity to provide the comparison between the computer simulation results and the experimental data. At a higher level of low-voltage conductivity, the injected charge totally recombines in the near-electrode area and the intensity of EHD flow strongly decays up to reversing its direction. In this case, the dissociation (conductivity) must be taken into account.

2.3.3 The field-enhanced dissociation

As known (Plumley, 1941; Onsager, 1934; McIlroy and Mason, 1976), the intensity of the dissociation should grow under the influence of the strong electric field. Such

enhancement is often called the Wien effect, and some researchers believe the effect to underlie the space charge formation in the low-conducting liquids and to lead to the EHD flow emergence. To provide the investigation of the features of high-voltage current passage in the case of the Wien effect, our computer model was supplemented with the explicit dependence of the dissociation rate on the electric field strength. Besides, to simplify the analysis, the injection charge formation was omitted from consideration.

Major results obtained in this model are presented in (PII; AIII). The following conclusions are made in them:

- both the dissociation and injection mechanisms of charge formation under identical external conditions can lead to emergence of EHD flows with the same direction, similar structure and intensity;
- the structure and intensity of EHD flows caused by the Wien effect is strongly dependent on the applied voltage as opposed to the case of the injection charge formation;
- a highly intensive EHD flow is more stable in the case when caused by the field-enhanced dissociation as distinct from the injection since in the latter case fluctuations of the lateral boundary of the charged area and corresponding instabilities of the flow are observed;
- EHD flows can in fact emerge at a higher level of low-voltage conductivity due to the Wien effect unlike the case of injection.

Fig. 8 shows specific distributions of the fluid velocity and space charge density obtained in the model of field-enhanced dissociation. As can be seen, the distributions actually have a number of similarities with those under the injection model. Namely, the obtained EHD flow is directed away from more pointed electrode to blunter one and is localized within a narrow central jet where the charge of the same polarity as the needle electrode is concentrated. A slight difference between the compared models consists in the presence of a thin layer of heterocharge located along the needle surface.

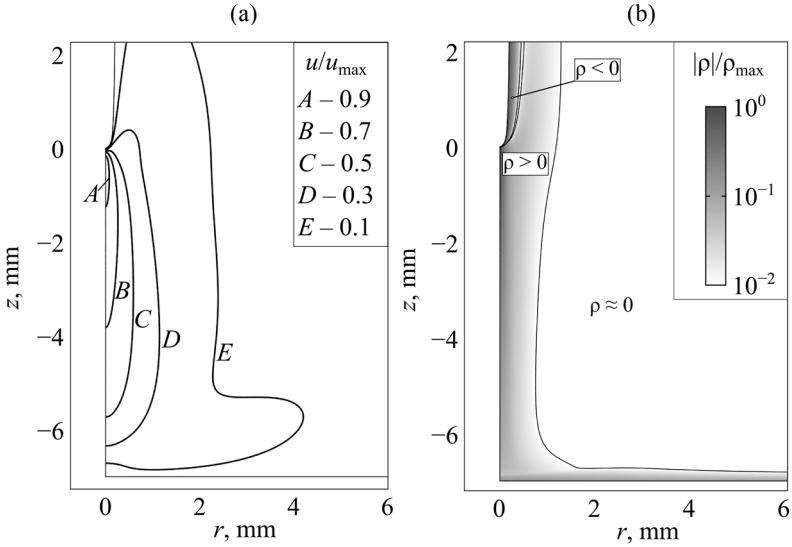

FIGURE 8 (a) The contour plot of the fluid velocity and (b) the absolute value of space charge density on a logarithmic scale at $\sigma_0 = 10^{-9}$ S/m and $\varphi_0 = 10$ kV.

Conduct the qualitative comparison of the steady-state axial distributions of the space charge density and fluid velocity in two models of charge formation and consider the case of approximately equal flow rates (Fig. 9). Presented plots allow concluding that in spite of some differences, the general structures have a number of similarities. Thus, the space charge density distributions in both models show the considerable decay along the axial path with the maximum value attained near the surface of the needle electrode, and the view of velocity distributions in two cases is also similar. The presence of a very thin heterocharge layer near the needle surface and the slightly steeper decrease of the space charge density along the axis are two minor distinctions of the field-enhanced dissociation model from the injection one. Though the latter distinction leads to the absence of the zone of quasi-uniform flow along the axis, it actually has no influence on the general velocity distribution in all the bulk, since it is the viscous force that causes the fluid motion outside the charged jet in both models. Moreover, if the low-voltage conductivity is taken into account in the injection model, the corresponding EHD flow structure becomes even more similar to the one in the model of field-enhanced dissociation. Therefore, revealing the differences between the EHD flow structures in cases of the injection into low-conducting liquid and the Wien effect occurrence calls for further investigation.

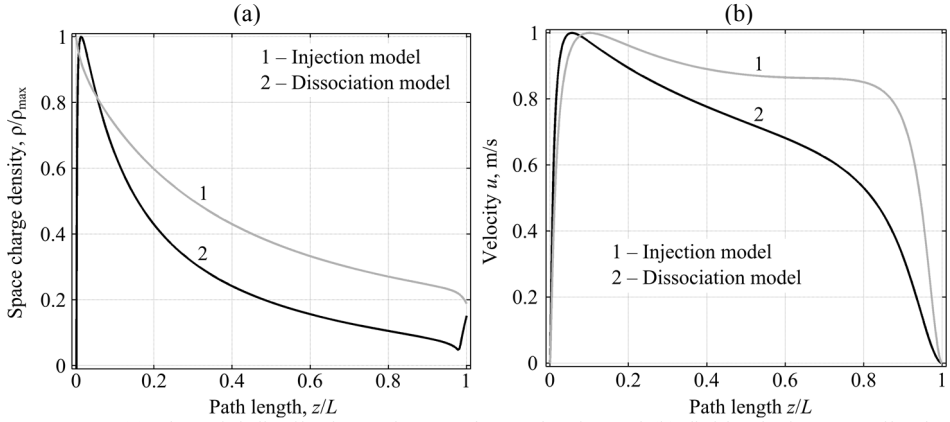

FIGURE 9 (a) The axial distributions of space charge density and (b) fluid velocity normalized to the maximum value in the injection model and field-enhanced dissociation one (φ_0= 10 kV).

Thus, it can be concluded that such qualitative similarity of the EHD flow structures under two mechanisms of charge formation makes it difficult to ascertain the prevailing one. It may be expected though that the Wien effect will play a more significant role in the emergence of EHD flow at both the heightened voltage and conductivity (about $\sigma_0 = 10^{-9}$ S/m and higher). Accordingly, at the lower conductivity level and moderate electric field strength EHD flows should be caused by the injection mechanism of charge formation. And in the intermediate case, the simultaneous influence of both mechanisms is to be expected. Thus, there are ranges where the only one mechanism prevails and a range where they have a similar significance.

2.4 Current–voltage and current–time characteristics

Presented above are the spatial (local) distributions of the required functions within the cell, which were used to conduct analysis of the structure and reveal the features of EHD

flows under two mechanisms of charge formation. Yet, it is the integral characteristics (in particular, current–voltage and current–time ones) that are of great interest since they can be obtained in the experiment and they are easy-to-use to describe system properties as a whole. The numerical experiments let one investigate the shape of CVC and CTC and interrelate their features with processes taking place inside the bulk. Besides, the computer simulation makes it possible to detect salient features of CVC in all cases of charge formation considered above and attempt to reveal similar ones in the appropriate experimental data.

2.4.1 Current–time characteristics

To calculate the total value of the electric current passing through the external electrical circuit in the steady-state regime, it is enough to integrate the current density over the surface of either electrode. However, when considering the unsteady case, the instantaneous current passed by any electrode fails to be proportional to the number of ions received by it per second, since the ions moving in the bulk without reaching the electrode surfaces change the polarization charge at the electrodes, thereby inducing an additional electric current (Shockley, 1938; Ramo, 1939). Consequently, the total current in this case is the sum of the integral of the current density over the electrode surface and the polarization current.

There are several ways to calculate the total current, but the most convenient and reliable one is the approach based on the Shockley–Ramo theorem (Shockley, 1938; Ramo, 1939; Hamel and Julien, 2008). According to the latter, the total current running through the external electric circuit is given by:

$$I = \int_V \left(\overrightarrow{J_{\mathrm{el}}}, \overrightarrow{f_{\mathrm{E}}}\right) d\vec{x}, \tag{12}$$

where $\overrightarrow{J_{\mathrm{el}}}$ is the electric current density and $\overrightarrow{f_E}$ is the weighting electric field (in units of inverse distance) (Hamel and Julien, 2008).

If the voltage across the gap varies the capacitive current will run and the specific additional term has to be included in Eq. (12):

$$I = \int_V \left(\overrightarrow{f_{\mathrm{E}}}, \overrightarrow{J_{\mathrm{el}}}\right) d\vec{x} + \varepsilon\varepsilon_0 \frac{\partial \varphi}{\partial t} \int_V \left(\overrightarrow{f_{\mathrm{E}}}, \overrightarrow{f_{\mathrm{E}}}\right) d\vec{x}. \tag{13}$$

The specific feature of Eq. (12) is that the contribution of the convective, diffusive and migration mechanisms of charge transport to the total value of the current flowing through the external electric circuit can be considered separately if the current density is represented as the sum of its components.

The main results of computer simulation of CTC are presented in the included article (PIV). The following conclusions are drawn there.

Calculated CTCs are in agreement with the aggregate of various experimental data presented in the literature, however, the computer simulation makes it possible not only to describe but also to explain the features of unsteady integral current characteristics. The shape of *I–t* characteristic is dependent on mechanisms of charge formation, the ratio of the initial and stationary ion concentrations and the mechanisms of charge transport. The initial current level (at the first instant after the application of the voltage) is conditioned by the initial ion concentration. Thus, since there are no ions in the pure injection model before the voltage turn-on, the current starts to grow from the zero level. And the initial current is equal to the conduction one in the dissociation model. The current behaves

(increases or decreases), depending on the ratio of the initial and stationary ion concentrations. If high-voltage mechanisms of charge formation activate after the application of the voltage, the ion concentration increases in the bulk, and the current becomes stronger. And if the charge formation is independent of the electric field (e.g., in the case of constant intensity of dissociation), the ion concentration decreases due to the charge loss on electrodes, and the current drops.

The shape of CTC in the high-voltage range is caused by both the drift of ions and their convective motion provided by EHD flow, therefore the determination of the ion mobility by the shape of CTC is to be justified in every case while it is ignored in a number of papers. The convective charge transport accelerates the transient process, reduces the time of attaining the steady-state electric current value, and also intensifies the removal of charge from the electrode, which thereby decreases the degree of the electric field screening. Moreover, in the injection model, it is the instabilities of EHD flows that cause electric current fluctuations in the case of strong injection (PII). And in the opposite case of weak injection, the maximum of the electric current corresponds to the instant when the EHD jet reaches the counter electrode.

Among other things, the high rate of transient processes is to be noted. It considerably complicates the experimental study of CTCs and interpretation of already obtained results especially if one takes into account the high complexity of getting voltage-step with rising edge shorter than the specific time span of the EHD flow formation.

2.4.2 Dynamic current–voltage characteristics

Both the experimental (e.g., Stishkov and Ostapenko, 1989; Zhakin, 2003; Daaboul et al., 2009) and the theoretical research (e.g., Grosu et al., 2007; Denat, 2011) concerning CVCs of dielectric liquids took place during the last several decades and a great amount of data was accumulated. In spite of the apparent simplicity of such experimental study, getting the CVCs of low-conducting liquid is linked with a number of difficulties such as high duration of transient processes, strong current fluctuations caused by instabilities of EHD flows, etc. A new approach to measuring the integral current characteristics devoid of most such shortcomings was suggested in (Stishkov and Ostapenko, 1989). It consists of studying the current-voltage characteristics obtained under dynamic conditions, i.e., with the voltage modulation by a saw-tooth signal. Corresponding data are referred to as dynamical current-voltage characteristics or DCVCs.

The main advantage of the method is the rapidity of the experimental data acquisition as the whole measuring process goes on under constant external conditions. Besides, using the DCVC method makes it possible to verify the reproducibility of the characterization as opposed to the classical method where the same verification is very time-consuming. In spite of a number of advantages, the application of DCVC has been restricted until now since the obtained result was dependent on the rate of voltage modulation, the two parts of DCVC corresponding to increasing and decreasing voltage had differences (i.e., the so-called hysteresis), and the capacitive current distorted the experimental oscillograms. However, the suggested method for computer simulation of the current passage processes in low-conducting liquids with the subsequent determination of the integral current characteristics lets one obtain DCVC as a result of the numerical calculation. And this makes it possible to analyze the specificity of DCVC in different

models of charge formation, interpret experimentally revealed features and resolve all contradictions.

The general results of computer simulation of dynamical current-voltage characteristics are presented in (AII; AX). Consider the most typical of them and analyze the shape of calculated DCVC. Fig. 10*a* shows corresponding results obtained in the following cases: the pure dissociation (without the injection and the Wien effect) and the injection into non-conducting and low-conducting liquids. The case when the conduction and injection currents are of the same order of magnitude is chosen for the comparison. Presented data are calculated at the voltage modulation rate of 20 kV/s.

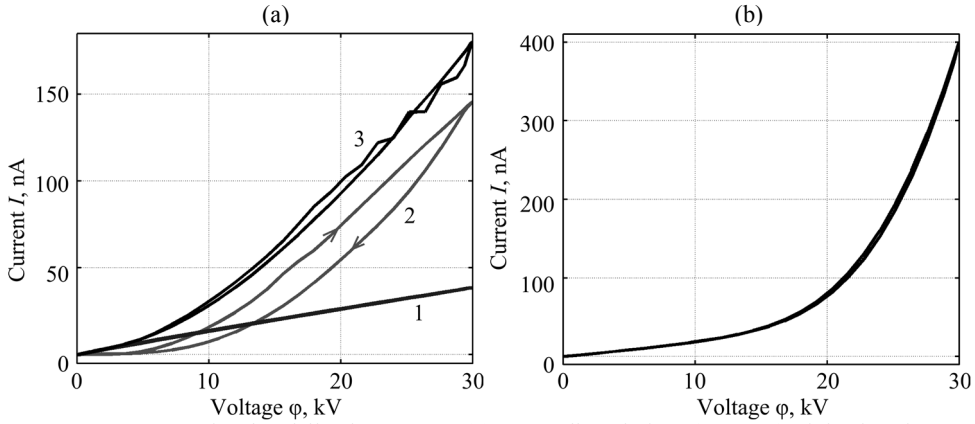

FIGURE 10 DCVC in the following cases: (a) pure dissociation (curve 1), injection into non-conducting and low-conducting liquids (curves 2 and 3, respectively) and (b) field-enhanced dissociation (at $\sigma_0 = 10^{-10}$ S/m).

The curve 1, i.e., DCVC in the pure dissociation model (without the Wien effect), is practically linear in the considered voltage range and shows no hysteresis as distinct from the curve 2. The latter one, i.e. DCVC in the pure injection model (without dissociation), begins to rise only after the activation of the injection (thereby failing to describe the low-voltage part of CVC) with the increasing voltage section being higher than the decreasing voltage one. This difference (as shown in AII) is caused by the reduction of the intensity of injection charge formation due to growth of the electric field screening under the influence of the space charge density accumulated in the bulk over the first half of the voltage modulation period.

The curve 3 obtained in the joint model (taking into account both injection and dissociation, though without the Wien effect) coincides with the curve 1 in the low-voltage range (up to 5 kV) and shows the current growth to begin immediately after the onset threshold of EHD flows. One can say this DCVC represents almost the sum of two previous ones (simulated in models where each mechanism of charge formation was considered separately) except for the absence of hysteresis. This distinction is explained by the facilitation of the neutralization of the excessive space charge density in the presence of low-voltage conductivity, which, in turn, leads to the reduction of the electric field screening and lessening the difference between the corresponding values under the increasing and decreasing voltages.

Fig. 10*b* shows DCVC calculated in the model of field-enhanced dissociation. Unlike the one obtained in the model of the injection into low-conducting liquid, this

DCVC is linear in a wider voltage range—approximately up to 15 kV when the local electric field strength at the needle tip reaches the value about 10^8 V/m. Further voltage increase leads to the steeply rising current with its peak magnitude being 10 times the corresponding value of the current in the dissociation model without the Wien effect. Moreover, there is no hysteresis in this model despite a quite high current level.

So, the conducted simulation made it possible to explore features of DCVC and to establish the interrelation between them and mechanisms of charge formation and ion transport. Results of numerical calculations showed the hysteresis of DCVC obtained experimentally earlier to be caused by a drop in the injection intensity at the voltage decrease due to the electric field screening in near-electrode area under the influence of the space charge accumulated in the bulk.

2.5 Experimental results

The visualization and recovery of the velocity field of three-dimensional EHD flows presents a complicated problem and, moreover, lets one obtain only rather limited set of data. Nevertheless, the experimental research of EHD flows is needed to verify the computer simulation results, validate the choice of various calculation parameters and expand understanding of the subject. Besides, the shortage of experimental data in needle–plane type systems utilized in practical devices like EHD pumps or atomizers (Funakawa and Balachandran, 2009; Shrimpton, 2009a) imparts a special interest to the present study. Also, it is worth noting that a feature of the present experimental investigation lies in that it is carried out jointly with numerical calculations, thereby providing an opportunity to improve physical and computer models of EHD flows.

2.5.1 General results

The main experimental results are presented in the included articles (PI; PIII) and in (AIII; AIV). To begin with, consider a typical example of processed tracks with velocity vectors along them (Fig. 11*a*) and the velocity distribution along a track (Fig. 11*b*) in purified transformer oil under +12 kV voltage. The schematic drawing on the right-hand side of Fig.11*b* shows the track being used to build the presented velocity line chart. Two vertical lines on the latter correspond to cross points between the chosen track and the boundary of specified area designated on the schematic drawing.

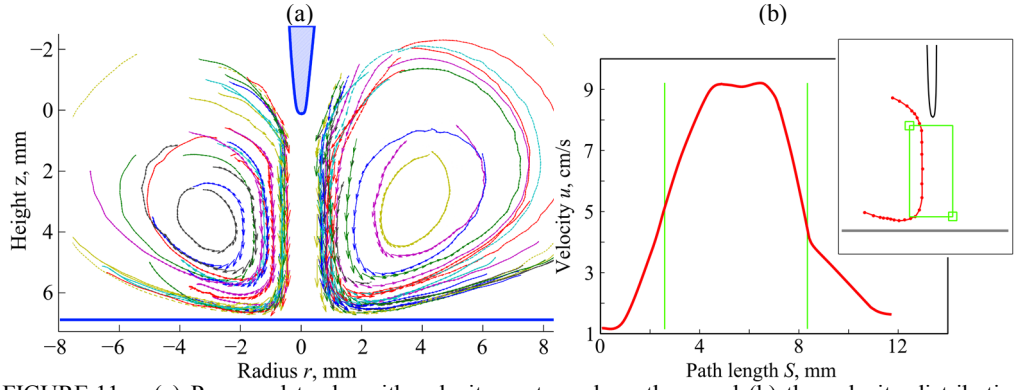

FIGURE 11 (a) Processed tracks with velocity vectors along them and (b) the velocity distribution along the chosen track at +12 kV voltage.

Fig. 11*a* displays, in particular, the typical number of investigated tracks for one voltage value and the area of their localization. In spite of processing a great amount of data, we have failed to find any trajectory of visualization particle (in all data sets) in the immediate vicinity of the model axis, i.e., in the area of the most intense flow. Apparently, this is due to the ejection of air bubbles from near-electrode area of reduced pressure.

The shape of particle tracks lets one define characteristic zones of a flow. Thus, the area where lines are drawn together to form a cone-shaped structure is the acceleration zone. The one where velocity vectors are directed along the symmetry axis is the zone of the uniform flow. The area of line divergence corresponds to the deceleration zone. The right-hand plot lets one estimate the magnitude of fluid acceleration. Thus, the fluid velocity increases up to 10 cm/s within a distance of several tenths of centimeter, which corresponds to the acceleration value of about 10 m/s^2. In addition, it can be seen that fluid begins to accelerate even above the needle tip.

Fig. 12*a* presents the characteristic contour plot of the velocity in the case of developed EHD flow. It agrees quite well qualitatively with the one obtained in the computer simulation excepting the narrow area along the model axis where no tracks were observed. Hence, the acceleration area seems to be more extended in the vertical direction.

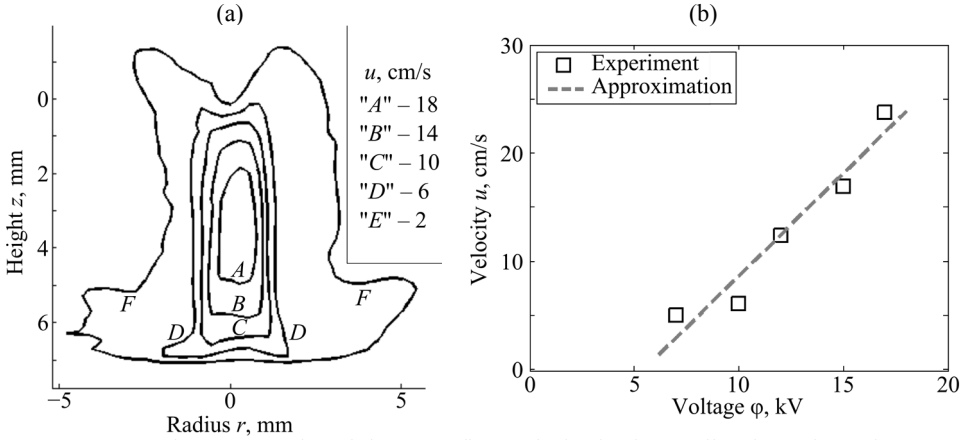

FIGURE 12 (a) The contour plot of the EHD flow velocity in the needle–plane electrode system in purified transformer oil under +17 kV voltage and (b) the voltage dependence of the average velocity in the middle of the interelectrode gap.

To provide correct recovery of the velocity value in the middle part of the jet, the curve fitting of corresponding cross-section distributions using the Pade approximant (i.e, with a rational function) was made. As a result of such postprocessing, the voltage dependence of the average velocity in the middle of the interelectrode gap was obtained (Fig. 12*b*). It shows the intensity of EHD flow to be linearly dependent on the voltage across gap, of course, within the accuracy of experimental data. The latter fact conforms to the typical data presented in the literature (e.g., Stishkov and Ostapenko, 1989). The obtained data also show the characteristic velocity of EHD flow in the liquid without special impurities to be comparably small—about a few tens of centimeters per second.

2.5.2 The comparison of the experimental data with computer simulation ones

Compare the experimental data with the simulation ones obtained in the computer model closely corresponding to the real one (in cell sizes, needle shape, liquid properties, etc.).

First of all, we have obtained the experimental current-voltage characteristic in the needle–plane electrode system, and have calculated it using several functional dependences. Fitting the coefficients in a relatively simple dependence (3) has allowed us to achieve the agreement between the experimental and calculated current-voltage characteristics over a wide voltage range (Fig. 13*a*). It is essential to note that even rather small (within 10%) variation in coefficients A, B causes a considerable difference between the experimental and the calculated CVCs, thereby accentuating the limitation of choice of the injection function form.

Then, the velocity distributions obtained in the experiment (using the PTV technique) and calculated numerically using the dependence $j_{inj}(E)$ were compared, and an example of the corresponding plots of the cross-section velocity distribution is shown in Fig. 13*b*. The difference between the plots lies within 10% except for the central part of jet where there were no trajectories of seeding particles in the experiment.

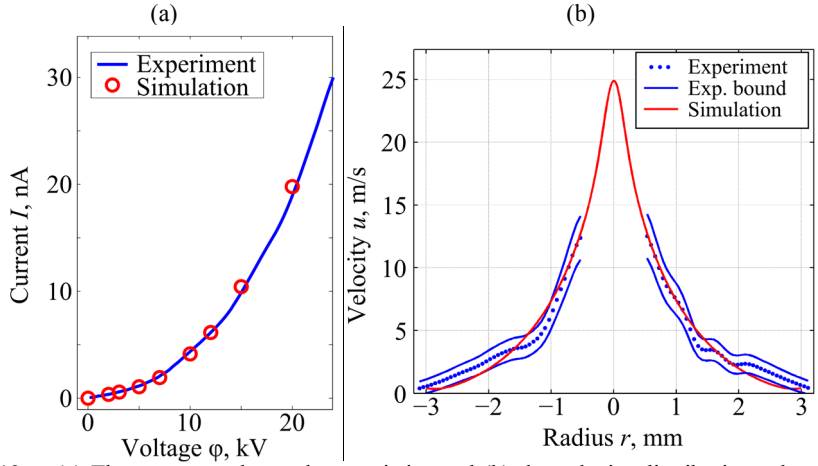

FIGURE 13 (a) The current–voltage characteristics and (b) the velocity distributions along the cross-section through the middle of the interelectrode gap obtained in the experiment and in the simulation at the voltage of 15 kV.

Fig. 14 presents corresponding velocity contour plots obtained in the experiment (on the left-hand side) and in the simulation (on the right-hand side) with velocity values being indicated in cm/s. On the whole, they have a similar shape taking into account complexities and errors of the experimental velocimetry method. A good agreement is seen for outward contours where many experimental tracks were recorded and processed and where thereby corresponding data have higher reliability.

Thus, the presented comparison lets one conclude that the chosen injection function describes in a quite good manner the process of charge formation for particular types of metal and liquid. This, in turn, shows the opportunity to use the experimentally fitted functional dependence of the injection current density on the electric field strength for simulation of EHD flows. Moreover, appropriate results of the computer simulation can be

considered as the immediate supplement of the experimental data, which, first of all, makes it possible to study distributions of those variables that cannot be found in the experiment (e.g., the space charge density, electric field strength, fluid pressure, etc.).

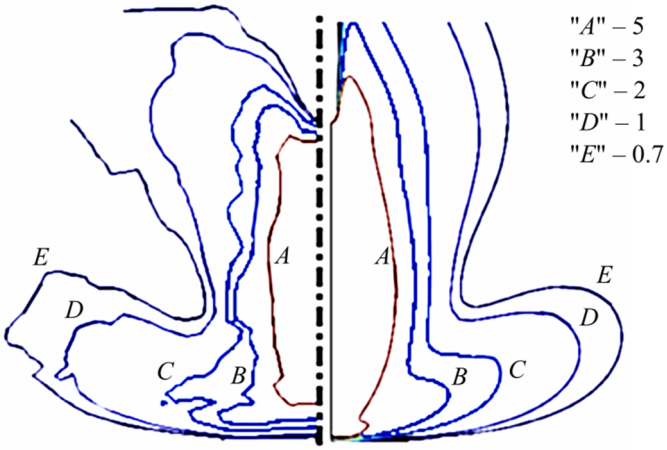

FIGURE 14 The contour plot of velocity obtained in the experiment (on the left-hand side) and in the simulation (on the right-hand side) at the voltage of 12 kV.

2.5.3 Features of EHD flow in the superstrong electric field

Investigation of EHD flows in the superstrong electric fields presents a particular interest. It is especially so in view of the fact that the Wien effect according to the theoretical description (6) is in the exponential dependence on the electric field strength and, therefore, should appear in full force in this case. The growth of the electric field non-uniformity in the present study was achieved by virtue of fine sharpening of the needle tip up to a radius of 3 μm. The purified petrolatum oil and the one with iodine were utilized as working liquids.

The main results of this investigation are presented in the included article (PIII) where the following conclusions are made. The emergence of the EHD flows in high-purity liquids with small low-voltage conductivity (like the petrolatum oil) is attended with a sharp increase of the current running through the liquid—from tens of picoamperes up to tens of nanoamperes, which occurred at a voltage of about 15 kV in the case under consideration. The analysis of the CVCs brings us to the conclusion that the corresponding growth of the current is independent of the voltage polarity and introduction of special impurities into the liquid, and takes place due to the Wien effect. Besides, the shape of obtained DCVCs (represented in AII and AX with the capacitive current having been excluded) is qualitatively similar to that calculated in the field-enhanced dissociation model, which also confirms our assumption.

2.6 Conclusions

Comprehensive and systematical research into high-voltage processes of the current passage through dielectric liquids in a wide voltage range (up to the breakdown) was carried out. Conducted investigations of EHD flows on the base of both the computer simulation and experimental study made it possible to gain more insight into their

behavior in different cases of charge formation. The emphasis was on the features of EHD processes in the case of high non-uniformity of the electric field distribution. Performed numerical calculations allowed us to describe kinematic, force and electric current structures of EHD flows and investigate the influence of charge formation mechanisms on them.

Achievements and findings:

1. A technique for computer simulation of EHD flows in liquids with a non-zero value of low-voltage conductivity is developed with a number of EHD problems having been solved on its base.
2. The issue of the prevailing mechanism of charge formation leading to the emergence of EHD flows is brought to a close, and it was shown that both injection and dissociation mechanisms of charge formation can prevail depending on conditions.
3. The zone of quasi-uniform velocity distribution in the central jet of EHD flow is shown to be specific only for the injection model, while the corresponding distribution in the field-enhanced dissociation model is non-uniform with the EHD flow structure strongly depending on the voltage.
4. A method for numerical calculation of the current-time characteristic and the dynamical current-voltage one was developed, and EHD flows under every mechanism of charge formation were shown to have a considerable effect on them.
5. A comparison of computer simulation results and the experimental data was carried out, and a satisfactory qualitative and quantitative agreement between them was observed.

Improvements and extensions:

1. Application of the developed method for computer-aided design of new EHD devices and optimization of the existing ones.
2. Conduction of detailed investigation of charge formation mechanisms proper and precise determination of limits of their prevalence.
3. Development of a method for ascertaining the prevalent mechanism of charge formation by the experimental data set.
4. Investigation of the influence of the ion mobility value on the structure and features of EHD flows.
5. Supplement of existing experimental methods for finding the electrophysical properties of liquids (e.g., the ion mobility and electric conductivity) with appropriate computer models based on the proposed simulation technique.

REFERENCES

Adamczewski, I. 1969. *Ionization, Conductivity and Breakdown in Dielectric Liquids*. Taylor and Francis Ltd., London.

Afanasyev, S. B., Lavrenyuk, D. S., Nikolaev, P. O., and Stishkov, Yu. K. 2007. A semiautomatic method for computer processing of the velocity profile in EHD flows. *Surface Engineering and Applied Electrochemistry*, 43(1), 18–23.

Apfelbaum, M. S. and Apfelbaum, E. M. 2001. One model of electric conduction and electric field distributions in a liquid insulator. *J. Electrostatics*, 50(2), 129–142.

Apfelbaum, M. S. and Yantovsy, E. I. 1977. On the force acting a needle electrode and flows caused by it. *Magnitnaya Gidrodinamika*, 4, 73–81. [in Russian]

Ashikhmin, I. A. and Stishkov, Yu. K. 2009. Structural features of EHD flows in wire-wire symmetric systems of electrodes. *Surface Engineering and Applied Electrochemistry*, 45(6), 471–479.

Ashikhmin, I. A. and Stishkov, Yu. K. 2012a. Effect of insulating walls on the structure of electrodynamic flows in a channel. *Technical Physics*, 57(9), 1181–1187.

Ashikhmin, I. A. and Stishkov, Yu. K. 2012b. Electrohydrodynamic injection converters. *Surface Engineering and Applied Electrochemistry*, 48(3), 268–275.

Ashikhmin, I. A. and Stishkov, Yu. K. 2012c. Physical principles of the injection EHD pumps design. In *Proceedings of the 8th ISEHD, Gdansk, Poland*, 51–55.

Atten, P. 1974. Electrohydrodynamic stability of dielectric liquids during transient regime of space-charge-limited injection. *Phys. Fluids*, 21(10), 1822–1827.

Bartnikas, R. 1994. *Engineering Dielectrics. Volume III. Electrical Insulating Liquids*. Philadelphia: ASTM.

Bologa, M. K., Grosu, F. P., and Kozhuhar, I. A. 1977. *Electrokovekciya i teploobmen (Electroconvection and Heat Exchange)*. Shtiinca, Chisinau. [in Russian]

Buyanov, A. V. and Stishkov, Yu. K. 2003. Kinematic structure of electrohydrodynamic flow in “wire-wire” and “wire over plane” electrode systems placed in a liquid. *Technical Physics*, 48(8), 972–977.

Buyanov, A. V. and Stishkov, Yu. K. 2004. Peculiarities in the structure of electrohydrodynamic through flow in a symmetric electrode system. *Technical Physics*, 49(8), 1075–1078.

Castellanos, A. 1998. *Electrohydrodynamics*. Springer, Wien.

Daaboul, M., Louste, C., and Romat, H. 2008. Electrohydrodynamical characteristics of a dielectric liquid flow induced by charge injection. In *Proceedings of the 16th ICDL, Poitiers, France*, 66–69.

Daaboul, M., Louste, Ch., and Romat, H. 2009. Measurements on charged plumes – influence of SiO_2 seeding particles on the electrical behavior. *IEEE Trans. Dielectr. Electr. Insul.*, 16(2), 335–342.

Denat, A. 2011. Conduction and breakdown initiation in dielectric liquids. In *Proceedings of the 17th ICDL, Trondheim, Norway*.

Elagin, I. A. and Stishkov, Yu. K. 2005. The investigation of the recombination area of symmetric-opposite EHD Flows. In *Proceedings of the 15th ICDL, Coimbra, Portugal*.

Elagin, I. A. and Stishkov, Yu. K. 2009. Peculiarities of EHD-flows in the case of unipolar injection in the system of electrodes of the wire-plane type. *Vestnik Sankt-Peterburgskogo Universiteta Ser. 4 (Physics and Chemistry)*, 2, 31–40. [in Russian with English summary]

Felici, N. J. 1971. D.C. conduction in liquid dielectrics (Part II): Electrohydrodynamic phenomena. *Direct Current*, 2(4), 147–164.

Feng, Y. and Seyed-Yagoobi, J. 2007. Electrical charge transport and energy conversion with fluid flow during electrohydrodynamic conduction pumping. *Phys. Fluids*, 19(5), 057102/11.

Frenkel, J. 1938. On pre-breakdown phenomena in insulators and electronic semi-conductors. *Physical Review*, 54(8), 647–648.

Funakawa, T. and Balachandran, W. 2009. New electron injection technique for generating electrospray. In *Proceedings of the 7th ISEHD, Sarawak, Malaysia*.

Glushchenko, P. V. and Stishkov, Yu. K. 2007. Modeling of the through EHD-flow structure in a wire-wire system. *Surface Engineering and Applied Electrochemistry*, 43(4), 257–264.

Gogosov, V. V. and Polyansky, V. A. 1976. Electrohydrodynamics: problems and applications, general equations, discontinuous solutions. *Itogi Nauki i Tehniki. Mehanika Gidkosti i Gasa*, 10, 5–72. [in Russian]

Grosu, F. P., Bologa, M. K., Bloshchitsyn, B. B., Stishkov, Yu. K., and Kozhevnikov, I. V. 2007. Charge formation in liquid dielectrics under the influence of electrostatic field. *Surface Engineering and Applied Electrochemistry*, 43(5), 318–335.

Hamel, L.-A. and Julien, M. 2008. Generalized demonstration of Ramo's theorem with space charge and polarization effects. *Nucl. Instrum. and Methods in Phys. Res. A*, 597, 207–211.

Higuera, F. J. 2000. Electrohydrodynamic flow of a dielectric liquid around a blade electrode. *Phys. Fluids*, 12(11), 2732–2742.

Higuera, F. J. 2002. Electrohydrodynamic flow of a dielectric liquid due to autonomous injection of charge by a needle electrode. *Phys. Fluids*, 14(1), 423–426.

Hopfinger, E. J. and Grosse, J. P. 1971. Charge transport by self-generated turbulence in insulating liquids submitted to unipolar injection. *Phys. Fluids*, 14(8), 1671–1682.

Jeong, S. and Seyed-Yagoobi, J. 2002. Experimental study of electrohydrodynamic pumping through conduction phenomenon. *J. Electrostatics*, 56, 123–133.

Koulova, D., Perez, A., Traore, Ph., and Romat, H. 2008. Influence of the dielectric force on thermoelectric convection phenomena in case of weak injection. In *Proceedings of the 16th ICDL, Poitiers, France*, 110–113.

Kourmatzis, A. and Shrimpton, J. S. 2012. Turbulent three-dimensional dielectric electrohydrodynamic convection between two plates. *Journal of Fluid Mechanics*, 696, 228–262.

Landau, L. D. and Lifshitz, E. M. 1987. *Course of Theoretical Physics. Vol. 6: Fluid Mechanics*, 2nd edition. Butterworth-Heinemann, Oxford.

Lastow, O. and Balachandran, W. 2006. Numerical simulation of electrohydrodynamic (EHD) atomization. *J. Electrostatics*, 64, 850–859.

Lazarev, A. S. and Stishkov, Yu. K. 2006. Features of flows with allocated bulk force. In: *Proceedings of 8th MPEEL, St. Petersburg, Russia*, 60–65. [in Russian]

Lewin, P. L., Wang, P., Swaffield, D. J., and Chen, G. 2008. A model for bubble motion in non-uniform electric fields. In *Proceedings of the 16th ICDL, Poitiers, France*, 50–53.

Louste, C., Daaboul, M., and Romat, H. 2008. Experimental study of a plane turbulent wall jet induced by a dielectric barrier injection in dielectric liquid. In *Proceedings of the 16th ICDL, Poitiers, France*, 106–109.

McIlroy, D. K. and Mason, D. P. 1976. Wien dissociation in very low intensity electric fields. *J. Chem. Soc., Faraday Trans. 2*, 72, 590–596.

Melcher, J. R. 1981. *Continuum Electromechanics*. Cambridge: MIT Press.

Onsager, L. 1934. Deviations from Ohm's law in weak electrolytes. *J. Chem. Phys.*, 2, 599–615.

Ostroumov, G. A. 1979. *Vzaimodeistvie elektricheskih i gidrodinamicheskih polei: fizicheskie osnovy elektrogidrodinamici (Interaction of Electric and Hydrodynamic Fields: Physical Principles of Electrohydrodynamics)*. Nauka, Moscow. [in Russian]

Pankratieva, I. L. and Polyansky, V. A. 1995. Simulation of electrohydrodynamical flows in low-conducting liquids. *Prikladnaya Mehanika i Tehnicheskaya Fizika*, 36(4), 36–43. [in Russian]

Pankratieva, I. L. and Polyansky, V. A. 2006. Electrization of low-conducting multi-component liquids at laminar flowing in a plane channel. *Fiziko-Himicheskaya Kinetika v Gazovoi Dinamike*, 4, 248–260. [in Russian]

Perez, A. T. and Castellanos, A. 1989. Role of charge diffusion in finite-amplitude Electroconvection. *Physical Review A*, 40(10), 5844–5855.

Perez, A. T., Traore, Ph., Koulova-Nenova, D., and Romat, H. 2008. Numerical modeling of a two-dimensional electrohydrodynamic plume between a blade and a flat plate. In *Proceedings of the 16th ICDL, Poitiers, France*, 44–47.

Perez, A. T., Vazquez, P. A., and Castellanos, A. 1995. Dynamics and linear stability of charged jets in dielectric liquids. *IEEE Transactions on Industry Applications*, 31(4), 761–767.

Plumley, H. J. 1941. Conduction of Electricity by Dielectric Liquids at High Field Strengths. *Phys. Review*, 59, 200–207.

Polyansky, V. A. and Pankratieva, I. L. 1999. Electric current oscillations in low-conducting liquids. *Journal of Electrostatics*, 48(1), 27–41.

Raffel, M., Willert, C. E., Wereley, S. T., and Kompenhans, J. 2007. *Particle Image Velocimetry: a Practical Guide*, 2nd edition, Springer, Berlin.

Ramo, S. 1939. Currents induced by electron motion. In *Proc. of the IRE*, 27, 584–585.

Schneider, J. M. and Watson, P. K. 1970. Electrohydrodynamic stability of space-charge-limited currents in dielectric liquids. I. Theoretical study. *Phys. Fluids*, 13(8), 1948–1954.

Shelistov, V. S., Petrov, A. V., and Zhuzha, M. M. 2012. On electroconvection regimes. In *Proceedings of 10th MPEEL, St. Petersburg, Russia*, 91–92. [in Russian with English summary].

Shockley, A. 1938. Currents to conductors induced by a moving point charge. *J. Appl. Phys.*, 9, 635–636.

Shrimpton, J. 2009a. Charge injection electrostatic atomization. In *Proceedings of the 7th ISEHD, Sarawak, Malaysia*.

Shrimpton, J. 2009b. *Charge Injection Systems: Physical Principles, Experimental and Theoretical Work*. Springer, Berlin.

Stishkov, Yu. K. 1986. Ionization-recombination mechanism of charge formation. *Doklady Akademii Nauk*, 288(4), 861–865. [in Russian]

Stishkov, Yu. K. and Baranovsky, L. L. 1983. Drop method of the investigation of space charge in electroinsulating medium. *Magnitnaya Gidrodinamika*, 2, 137–140. [in Russian]

Stishkov, Yu. K. and Elagin, I. A. 2005. Simulation of nonstationary electrohydrodynamic flows in a symmetric system of electrodes of the wire-wire type. *Technical Physics*, 50(9), 1119–1123.

Stishkov, Yu. K. and Elagin, I. A. 2009. Comparison of free convection and EHD-flows using computer modeling. In *Proceedings of the 7th ISEHD, Sarawak, Malaysia*.

Stishkov, Yu. K. and Ostapenko, A. A. 1979a. Dependence of intensity and efficiency on low-voltage conductivity of the liquid in electrodynamic flows. *Magnetohydrodynamics*, 15(1), 60–64.

Stishkov, Yu. K. and Ostapenko, A. A. 1979b. Two regimes of hydrodynamic flow in convective conductivity. *Magnetohydrodynamics*, 15(4), 396–401.

Stishkov, Yu. K. and Ostapenko, A. A. 1989. *Elektrogidrodinamicheskie techeniya v zhidkih dielektrikah (Electrohydrodynamic Flows in Liquid Dielectrics)*. Izdatelstvo Leningradskogo gosudarstvennogo universiteta, Leningrad. [in Russian]

Stishkov, Yu. K. and Samusenko, A. V. 2010. Electrohydrodynamics of liquids and gases: Similarities and distinctions. *Surface Engineering and Applied Electrochemistry*, 46(1), 27–39.

Stishkov, Yu. K., Buyanov, A. V., and Lazarev, A. S. 2005. Simulation of the electrohydrodynamic flow pattern in an asymmetric system of electrodes. *Technical Physics*, 50(5), 576–581.

Stishkov, Yu. K., Dernovsky, V. L., and Statuya, A. A. 2007. Modeling of nonstationary EHD flows in a wire-plane electrode system. *Surface Engineering and Applied Electrochemistry*, 43(3), 182–186.

Stishkov, Yu. K., Dernovsky, V. L., Bologa, M. K., Grosu, F. P., and Kozhevnikov, I. V. 2006. Influence of length of the interelectrode gap on kinematics of EHD flows. *Elektronnaya Obrabotka Materialov*, 42(6), 28–36.

Stuetzer, O. M. 1959. Ion drag pressure generation. *J. Appl. Phys.*, 30(7), 984–994.

Tobazeon, R. 1984. Electrohydrodynamic instabilities and electroconvection in the transient and A.C. regime of unipolar injection in insulating liquids: A review. *J. Electrostatics*, 15(3), 359–384.

Traoré, Ph. and Pérez, A. T. 2012. Two-dimensional numerical analysis of electroconvection in a dielectric liquid subjected to strong unipolar injection. *Phys. Fluids*, 24, 037102/23.

Traoré, Ph., Daaboul, M., and Louste, C. 2010. Numerical simulation and PIV experimental analysis of electrohydrodynamic plumes induced by a blade electrode. *J. Phys. D: Appl. Phys.*, 43, 1–8.

Traoré, Ph., Koulova-Nenova, D., and Romat, H. 2005. Numerical approach of the electro-thermo-convective motion in a layer of a dielectric liquid. In *Proceedings of the 15th ICDL, Coimbra, Portugal*.

Van Dyke, M. 1982. *An album of fluid motion*. The Parabolic Press, Stanford.

Vazquez, P. A. and Castellanos, A. 2011. Stability analysis of the 3D electroconvective charged flow between parallel plates using the Particle-In-Cell method. In *Proceedings of the 17th ICDL, Trondheim, Norway*.

Vazquez, P. A., Georghiou, G. E., and Castellanos, A. 2006. Characterization of injection instabilities in electrohydrodynamics by numerical modelling: comparison of particle in cell and flux corrected transport methods for electroconvection between two plates. *J. Phys. D: Appl. Phys.*, 39, 2754–2763.

Vazquez, P. A., Georghiou, G. E., and Castellanos, A. 2008a. PIC-FE and FCT-FE numerical simulation of two-dimensional electroconvection: Comparison of the results. In *Proceedings of the 16th ICDL, Poitiers, France*, 29–32.

Vazquez, P. A., Georghiou, G. E., and Castellanos, A. 2008b. Transient evolution of finite amplitude electroconvection: scaling analysys. In *Proceedings of the 16th ICDL, Poitiers, France*, 90–93.

Watson, P. K., Schneider, J. M., and Till, H. R. 1970. Electrohydrodynamic stability of space-charge-limited currents in dielectric liquids. II. Experimental study. *Phys. Fluids*, 13(8), 1955–1961.

Yazdani, M. and Seyed-Yagoobi, J. 2010. The effect of charge injection on EHD conduction pumping. In *Proc. of the Industry Applications Society Annual Meeting (IAS)*, 1–5.

Zhakin, A. I. 2003. Ionic conductivity and complexation in liquid dielectrics. 45–61.

Zhakin, A. I. 2006. Near-electrode and transient processes in liquid dielectrics. *Phys. Usp.*, 49, 275–295.

Zhakin, A. I. 2012. Electrohydrodynamics. *Phys. Usp.*, 55, 465–488.

Zhakin, A. I., Kuzmenko, A. P., and Kuzko, A. E. 2012. Charge formation from the nanostructured metal surfaces at the electroconvection. *Izvestiya Yugo-Zapadnogo Gosudarstvennogo Universiteta*, 40(1/2), 60–71. [in Russian with English summary]

Zienkiewicz, O. C., Taylor, R. L., and Nithiarasu, P. 2005. *The Finite Element Method for Fluid Dynamics*. Elsevier, Oxford.